hsc70 was generated by reverse transcription-polymerase chain reaction (RT-PCR) from the mRNA obtained from the peripheral blood mononuclear cells (PBMCs) of a healthy volunteer. The total mRNA was extracted from the PBMCs with an Isogen kit (Wako, Osaka, Japan). The mRNA was transcribed to cDNA with oligo (dT) 16 primer using AMV reverse transcriptase (Promega, Tokyo, Japan). The cDNA encoding hsc70 was amplified by LA Taq polymerase (Takara, Tokyo, Japan) using the primers AT GGATCC C ATG TCC AAG GGA CCT G (forward) and AT GGTACC TTA ATC AAC CTC TTC AAT G (reverse). The amplified cDNA was cloned into a pQE31 expression vector (Qiagen, Tokyo, Japan) at 5' BamHI and 3' KpnI restriction sites. The hsc70/ESO p157-165 fusion protein was generated by incorporating a mini-gene encoding NY-ESO-1 p157-165 in either the forward or reverse primers containing the 5' *BamHI* and 3' *KpnI* restriction sites. *Escherichia coli* strain M15 was transformed by the constructed plasmids and grown in an Luria-Bertani (LB) medium, containing ampicillin (50 μg/ml) and kanamycin (20 μg/ml). Protein expression was induced by 0.1 M isopropyl-β-D-thiogalactoside (IPTG). The protein was solubilized in buffer B (8 M urea, 0.1 M sodium phosphate, 0.01 M Tris/ HCl, pH 8.0), the lysate was centrifuged of at 10,000 ×*g*, and the supernatant was applied to an Ni^{2+}-nitrilotriacetic acid (NTA) agarose column and extensively washed with buffer C (8 M urea, 0.1 M sodium phosphate, 0.01 M Tris/HCl, pH 6.3). The Ni^{2+}-NTA resin-bound 6× His-tagged protein was re-folded rapidly by washing with 15 column volumes of urea-free Tris buffer (pH 7.5) and eluted with Tris buffer containing 200 mM imidazole. The eluate was extensively dialyzed against phosphate buffered saline (PBS) (pH 7.4) to remove imidazole and then concentrated using an Amicon Ultra-15 centrifugal filter device (Millipore, Bedford, MA, USA). The fusion proteins were treated with Kurimover I and II (Kurita Incorporation, Tokyo, Japan) to remove the contaminating lipopolysaccharide (LPS). The level of LPS was determined by the Limulus ES-II test (Wako, Osaka, Japan).

Peptide. The human leukocyte antigen (HLA)-A0201 restricted NY-ESO-1 peptide p157-165 (SLLMWITQC) was identified by reactivity with cluster of differentiation 8 $(CD8)^+$ T-cell from patients with spontaneous NY-ESO-1 immunity. This epitope (ESO p157-165) was selected to analyze the $CD8^+$ T-cell response (17, 18). The peptide was synthesized by using the Multiple Peptide Systems, with a purity of >86%, as determined by reversed-phase high-performance liquid chromatography (HPLC).

Generation of dendritic cells from PBMCs. Mononuclear cells were isolated from the peripheral blood of healthy individuals by using Ficoll-Paque density gradient centrifugation after obtaining informed consent (19, 20). The $CD14^+$ monocytes were enriched by negative isolation using magnetic beads (Dynal, Oslo, Norway). Monocytes were seeded at a density of 1×10^6 cells/well in 24-well plates in 2 ml of RPMI 1640 medium with 2.5% or 10% fatal calf serum (FCS), 100 ng/ml granulocyte macrophage colony-stimulating factor (GM-CSF) (Leukine; Immunex, Seattle, WA, USA) and 50 ng/ml IL-4 (R&D Systems, Minneapolis, MN, USA). The culture was incubated at 37°C in a humidified atmosphere with 5% CO_2 for 5 days. The harvested cells were characterized by flow cytometry and were then stimulated with hsc70/ESO p157-165 fusion protein or p157-165 peptide.

Flow cytometry. The cells were processed for double-staining using fluorescein isothiocyanate (FITC)-CD14, FITC-CD1a, phycoerythrin (PE)-CD83, PE-HLA-DR, PE-CD86 (B7.2) monoclonal antibodies (mAbs) (BD Pharmingen, San Diego, CA, USA). Fluorescence acquisition was carried out on a FACSCan (BD Biosciences, San Diego, CA, USA), and data analysis was carried out using the CellQuest software package (BD Biosciences).

Stimulation of DCs and measurement of cytokines. The harvested cells were incubated with GM-CSF and IL-4 for 5 days and exposed to p157-165 (5 μg/ml) or hsc70/ESO p157-165 fusion protein (350 μg/ml) in RPMI 1640 for 12 h. The cell culture supernatants were collected and then particulates were removed by centrifugation. The concentration of the cytokines (IL-10 and 12) in the supernatants was measured by an enzyme-linked immunosorbent assay (ELISA; Quantikine, R&D Systems, Minneapolis, MN, USA).

Neutralization of IL-6 for differentiation of DCs from monocytes. mo-DCs were generated as described above. Anti-human IL-6 and/or IL-6R neutralizing antibodies, at a concentration of 2.5 μg/ml (R&D Systems), were added to the cultures at day 0 and 3 (21).

Results

Phenotype of mo-DCs from healthy donors. The population of monocytes isolated from PBMCs exhibited a unique phenotype (Figure 1a). However, the mo-DCs from the healthy donor were differentiated into two distinct phenotypes (Figure 1b). After 5 days, culture in RPMI, containing 10% FCS with GM-CSF and IL-4, the expression of CD14 was down-regulated in cells from half of the donors. On the other hand, CD1a was expressed in those cases. The expression of CD83 was negative in cells from all donors.

IL-10 production of mo-DCs from each donor. IL-10 was measured in the supernatants of DCs stimulated for 12 h by hsc70/ESO p157-165 fusion protein or p157-165 (Figure 2). $CD14^+CD1a^-$ DCs secreted significant amounts of IL-10 in response to hsc70/ESO p157-165 fusion protein. However, there was less IL-10 secretion stimulated by hsc70/ESO p157-165 fusion protein in $CD14^-CD1a^+$ DCs from donors 1 and 3.

The expression of CD1a and production of cytokines from mo-DCs. $CD14^-CD1a^-$ DCs (donor 5) produced IL-10, but IL-12, which plays a prominent role in the induction of the T-helper 1 (Th1) immune response against cancer, was barely secreted. Meanwhile, $CD14^-CD1a^+$ DCs from donor 6 exhibited a reversed pattern of cytokine production for IL-10 and IL-12 (Figure 3). The expression of surface markers CD14 and CD1a of mo-DCs had an effect on the balance of Th1 and Th2 response.

Mo-DCs from the same donor exhibited different surface marker phenotype after induction under different conditions. $CD14^-CD1a^+$ DCs were generated from donor 7 following

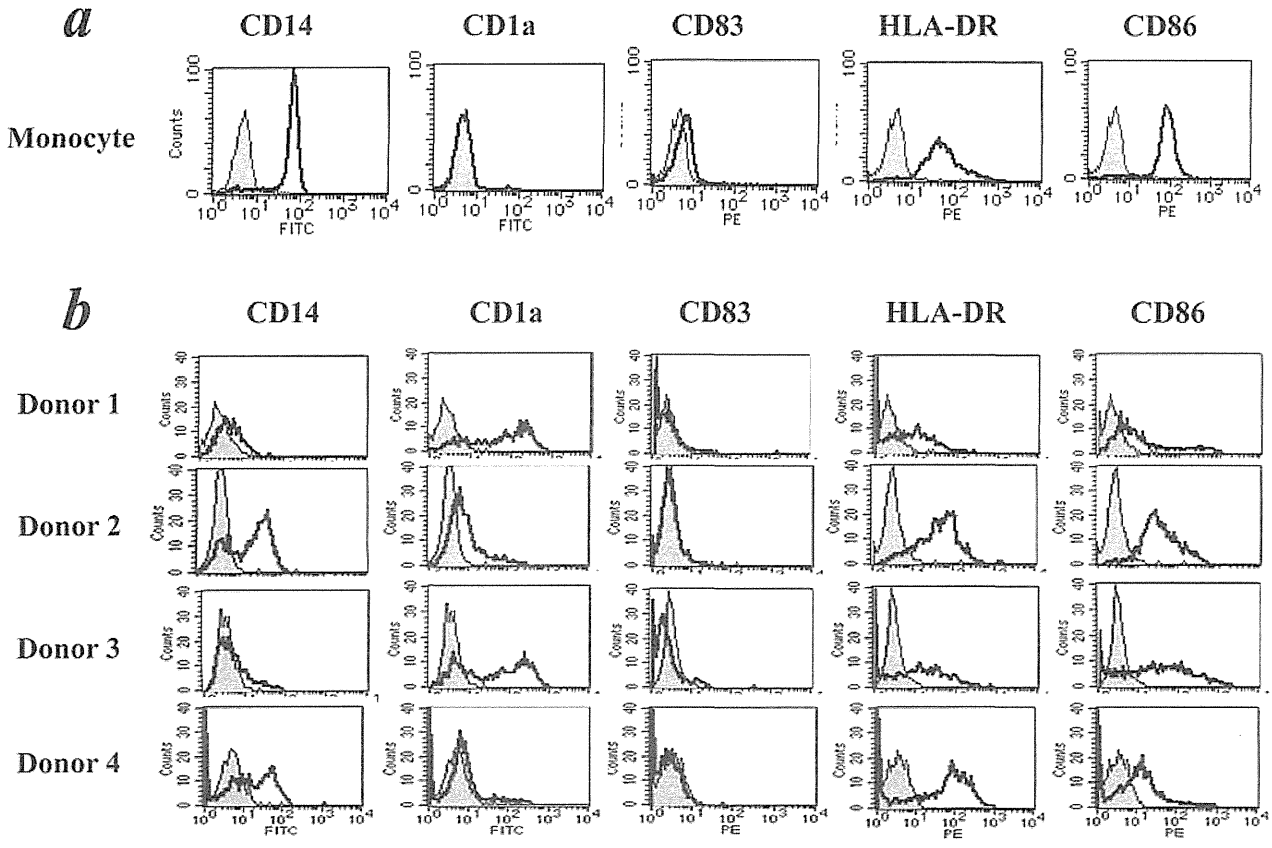

Figure 1. *a: Phenotype of monocytes isolated by magnetic beads from peripheral blood mononuclear cells. Cells were enriched and harvested immediately. b: Phenotype of monocyte-derived dendritic cells. Peripheral blood mononuclear cells were isolated from the peripheral blood of healthy individuals. The CD14+ monocytes enriched by negative isolation were incubated in RPMI plus 10% fetal calf serum, granulocyte macrophage colony-stimulating factor and interleukin-4, for 6 days. The phenotypes (CD14, CD1a, CD83, HLA-DR, CD86) of the harvested cells were analyzed by flow cytometry.*

culture in RPMI with 10% FCS. However, $CD14^+CD1a^-$ DCs were generated under culture conditions of RPMI with 2.5% FCS, using cells from the same donor. This phenotypic conversion changed the function of DCs, which exhibited IL-10 production rather than IL-12, in response to stimulation with hsc70/ESO p157-165 fusion protein (Figure 4).

The expression of CD1a and IL-6 antagonists. IL-6 affects the differentiation of monocytes into DCs and macrophages. The addition of IL-6 and/or IL-6R antibodies during the generation of mo-DCs up-regulated the expression of CD1a. The expression of CD1a was remarkable following blocking of both IL-6 and IL-6R (Figure 5). Although the DCs generated in medium containing 2.5% FCS were almost all $CD1a^-$ cells, the expression of CD1a was positive following the addition of neutralizing IL-6 and IL-6R antibodies on day 0 and 3. The function of the DCs differed according to their phenotypic features and they produced IL-12 in response to the activation by hsc70/ESO p157-165 fusion protein (Figure 6).

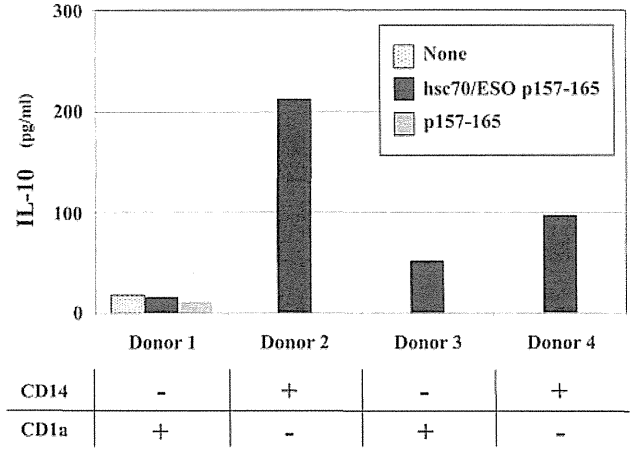

Figure 2. *Interleukin-10 (IL-10) production of dendritic cells (DCs). $CD14^-CD1a^+$ DCs and $CD14^+CD1a^-$ DCs were stimulated by hsc70/ESO p157-165 fusion protein or p157-165 in RPMI medium for 12 h. The IL-10 in the supernatants of pulsed DCs was measured by an enzyme-linked immunosorbent assay.*

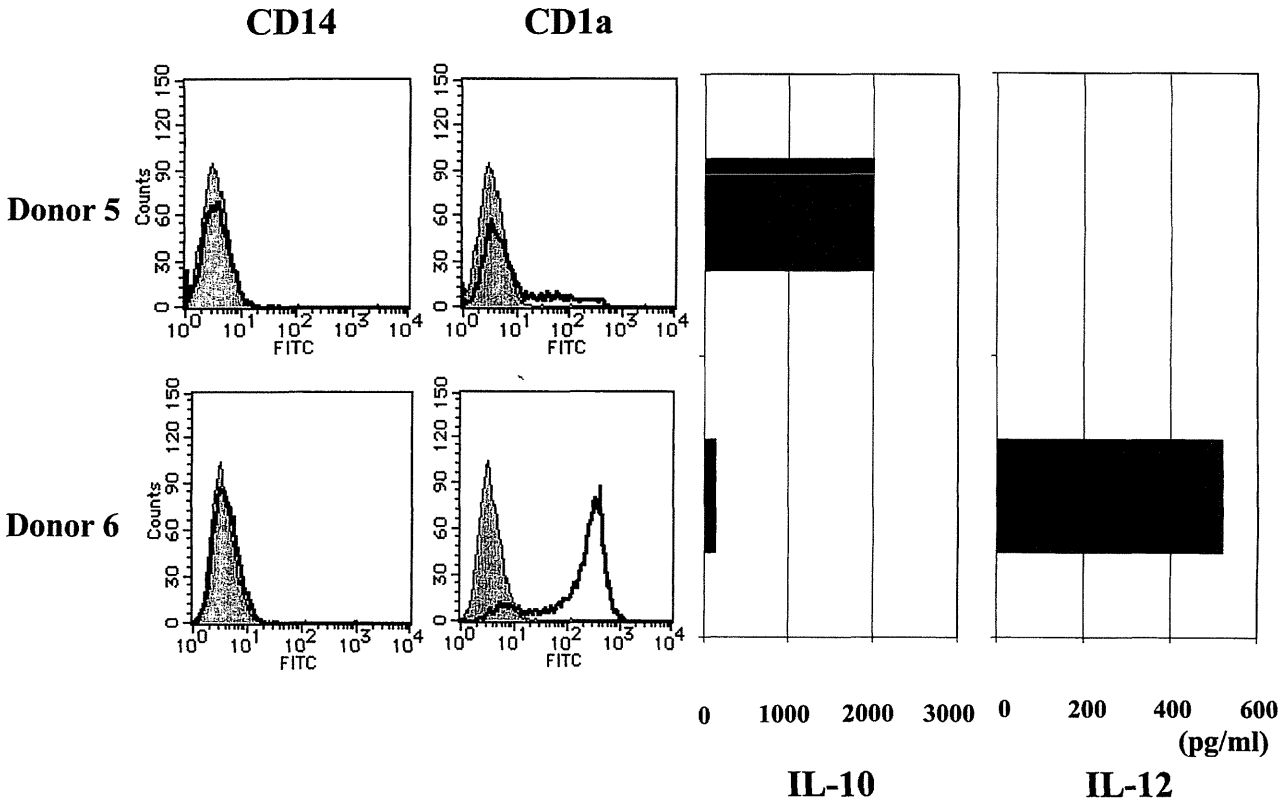

Figure 3. *Interleukin-10 (IL-10) and interleukin-12 (IL-12) production of dendritic cells (DCs). CD14$^-$CD1a$^+$ DCs and CD14$^+$CD1a$^-$ DCs were activated, as described in Materials and Methods by the hsc70/ESO p157-165 fusion protein. IL-10 and IL-12 in the supernatants of cells were measured by an enzyme-linked immunosorbent assay.*

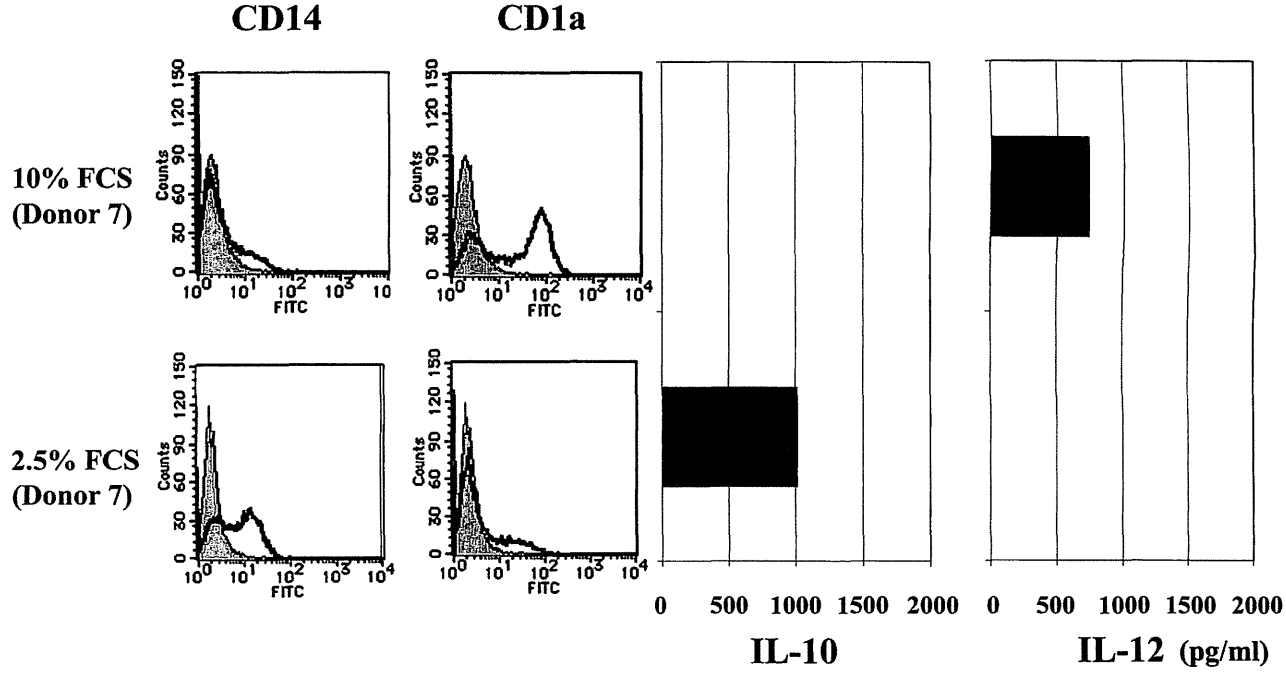

Figure 4. *Cytokine production of dendritic cells (DCs) in different culture medium. The percentage of fetal calf serum (FCS) in RPMI medium for generation of monocyte-derived DCs was changed from 10% to 2.5%.*

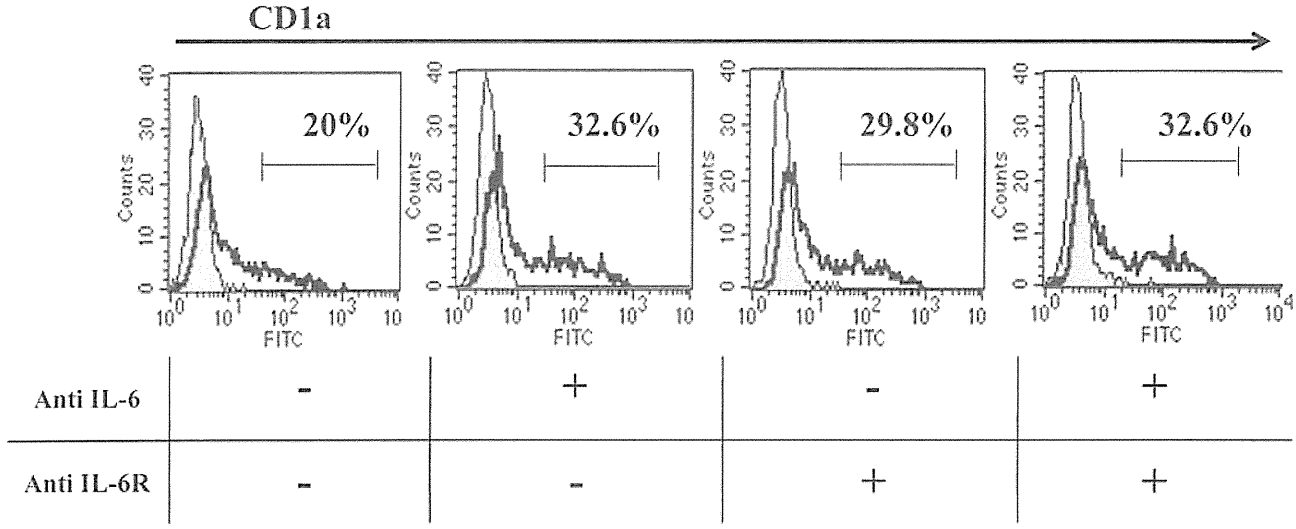

Figure 5. *The population of CD1a⁺ dendritic cells (DCs) after neutralizing Interleukin-6 (IL-6) and/or IL-6R. Antibodies to human IL-6 and IL-6R were added to the culture on day 0 and 3 of the generation of DCs from monocytes, in a medium with 2.5% fatal calf serum (FCS). The CD1a expression of harvested DCs was analyzed by flow cytometry on day 6.*

Discussion

NY-ESO-1 is a prototype cancer/testis antigen that is expressed in a variety of human malignancies, but not in normal tissues, except for the testis. Spontaneous immune responses involving an antibody, as well as $CD4^+$ and $CD8^+$ T-cells directed against a broad range of MHC class I- and class II-restricted NY-ESO-1 peptides are observed in patients with advanced NY-ESO-1-expressing tumors (22). Therefore, NY-ESO-1 is thought to be a favorable target for use as a cancer vaccine. The initial trials of peptide vaccination against NY-ESO-1 were particularly effective in generating $CD8^+$ T-cell responses. However, the clinical outcome remains unsatisfactory.

The major role of heat shock proteins (HSPs) is to act as a molecular chaperone, binding immature peptides during their synthesis and assisting in their folding (23-25). The peptides are thought to be degraded in the cytoplasm and are then transferred to the endoplasmic reticulum by binding to HSP70 or HSP90, but not by natural diffusion (26). In addition, HSPs are thought to bind to a diverse array of antigenic peptides in tumor cells, and that the tumor-derived HSP-antigenic peptide complexes can be purified for vaccination against cancer (27).

A mini-gene encompassing the NY-ESO-1 cytotoxic T-lymphocyte (CTL) epitope p157-165 (ESO p157-165) was genetically fused to the human heat shock cognate protein-70 (hsc70), and the resulting fusion proteins were expressed in *E. coli*. mo-DCs captured and endogenously processed the hsc70/ESO p157-165 fusion protein to MHC class I molecules through the cross-presentation pathway. Finally, NY-ESO-1-specific CTL were generated by *in vitro* stimulation with hsc70/ESO p157-165 fusion protein on mo-DCs.

DCs play a crucial role in the initiation of antigen-specific immune responses, exhibiting a variety of specializations that contribute to their efficiency as antigen-presenting cells (9, 28). One major population of DCs is myeloid DCs which include specific subtypes, including Langerhans cells, interstitial DCs and mo-DCs that have unique phenotypic features. The $CD14^+$ monocytes are the most common source of DCs and can be enriched by negative isolation from PBMCs and incubated in RPMI with 10% FCS, GM-CSF and IL-4 to generate DCs (29, 30). However, not all DCs generated or cultured under the same conditions are equivalent (31). They appear to be derived from multiple lineages and, depending on their origin, site of residence, or the type of maturation stimulus received, they program different T-cell outcomes (32). The generated mo-DCs exhibit various expression levels of CD1a, CD14, CD83, human leucocyte antigen-DR (HLA-DR) and CD86 according to the culture conditions and individuals from which they are sourced. mo-DC subsets are defined by their phenotypic features and have a functional diversity of cytokine production that regulates the polarization of naïve T-cells to Th1 or Th2 (33-36). However, this diversity creates difficulties in their clinical application in cancer immunotherapy using DCs. The optimal phenotypic features of DCs and appropriate conditions for clinical applications must be determined.

CD1a is one of the common DC subset markers (37, 38). The proportion of $CD1a^+$ and $CD1a^-$ DCs varies in individuals.

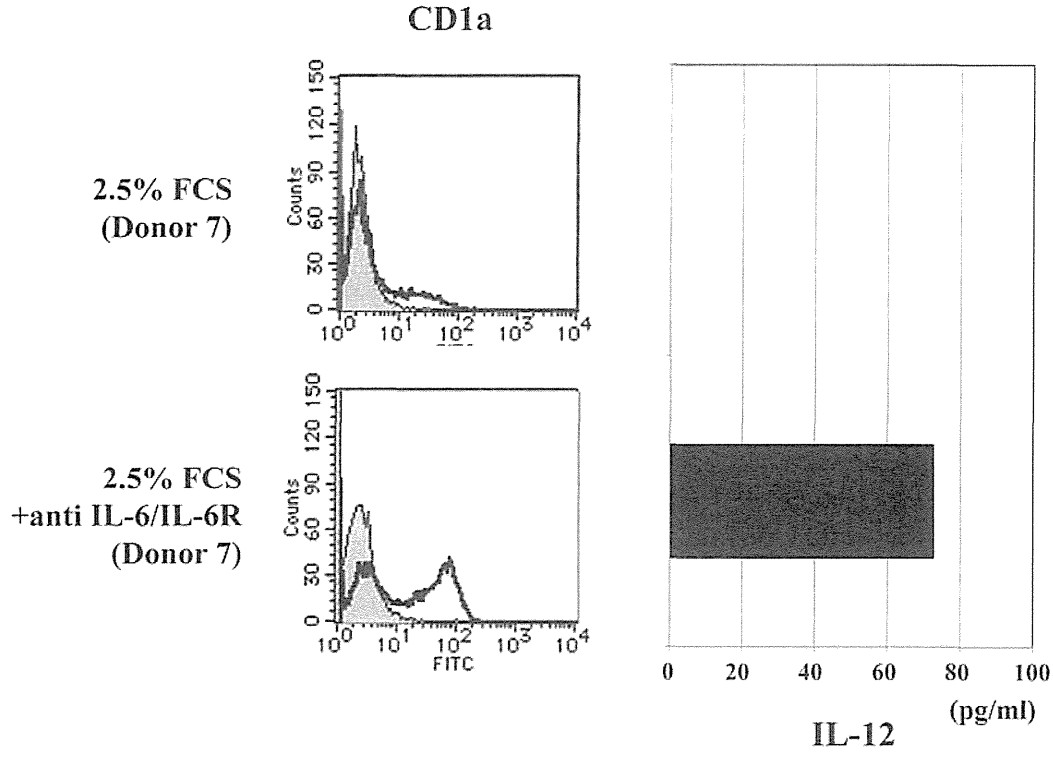

Figure 6. *Interleukin-12 (IL-12) production of monocyte-derived dendritic cells (mo-DCs) following culture with antibodies to interleukin-6 (IL-6) and IL-6R. The DCs generated in RPMI plus 2.5% fetal calf serum (FCS) and IL6/IL-6R antibodies up-regulated their expression of CD1a. The IL-12 production from DCs cultured with and without neutralizing IL-6 antibodies is shown.*

$CD1a^+$ DCs are able to secrete more IL-12 in response to stimulation with LPS than do $CD1a^-$ DCs. On the other hand, the IL-10 production of $CD1a^+$ DCs is less, or similar to that of $CD1a^-$ DCs (39). The present study generated two types of DCs, $CD1a^+$ and $CD1a^-$, under the same conditions. Interestingly, there were different patterns of CD1a expression under the different conditions during induction, even when using cells from the same donor. This strongly suggests that the conditions of DC culture were critical for induction of the appropriate antigen-presenting cells *in vivo*.

Humoral factors in the serum also affect the differentiation of immature DCs (40, 41). Culture medium with 2.5% FCS converted the phenotype of DCs from $CD1a^+$ to $CD1a^-$. This conversion also changed the cytokine production from IL-12 to IL-10. This is a critical conversion associated with the polarization of Th1 and Th2 cells. A major question was whether this conversion was reversible. IL-6 inhibits the differentiation of monocytes to DCs by promoting their differentiation toward macrophages (42, 43). On the other hand, an antagonist of IL-6 can drive monocytes to form immature DCs. Therefore, the present study compared the effect of anti-IL-6 agents on CD1a expression. Cells treated with both antibodies to IL-6 and IL-6R, recovered CD1a expression and secreted IL-12. These results suggest that anti-IL-6 analogs may be used as an effective adjuvant for the development of a mo-DC-based cancer vaccine with the hsc70/ESO p157-165 fusion protein.

Acknowledgements

This work was supported by a Grant-in-aid for Scientific Research on Priority Areas from the Ministry of Education, Culture, Sports, Science, and Technology of Japan (no. 16591263).

References

1 Caballero OL and Chen YT: Cancer/testis (CT) antigens: potential targets for immunotherapy. Cancer Sci *100*: 2014-2021, 2009.

2 Jager E, Stockert E, Zidianakis Z, Chen YT, Karbach J, Jager D, Arand M, Ritter G, Old LJ and Knuth A: Humoral immune responses of cancer patients against Cancer-Testis antigen NY-ESO-1: correlation with clinical events. Int J Cancer *84*: 506-510, 1999.

3 Scanlan MJ, Gure AO, Jungbluth AA, Old LJ and Chen YT: Cancer/testis antigens: an expanding family of targets for cancer immunotherapy. Immunol Rev *188*: 22-32, 2002.

4 Gnjatic S, Nishikawa H, Jungbluth AA, Gure AO, Ritter G, Jager E, Knuth A, Chen YT and Old LJ: NY-ESO-1: review of an immunogenic tumor antigen. Adv Cancer Res *95*: 1-30, 2006.

5 Jager E, Nagata Y, Gnjatic S, Wada H, Stockert E, Karbach J, Dunbar PR, Lee SY, Jungbluth A, Jager D, Arand M, Ritter G, Cerundolo V, Dupont B, Chen YT, Old LJ and Knuth A: Monitoring CD8 T cell responses to NY-ESO-1: correlation of humoral and cellular immune responses. Proc Natl Acad Sci USA *97*: 4760-4765, 2000.
6 Karbach J, Gnjatic S, Bender A, Neumann A, Weidmann E, Yuan J, Ferrara CA, Hoffmann E, Old LJ, Altorki NK and Jager E: Tumor-reactive CD8+ T-cell responses after vaccination with NY-ESO-1 peptide, CpG 7909 and Montanide ISA-51: association with survival. Int J Cancer *126*: 909-918, 2010.
7 Old LJ: Cancer vaccines: an overview. Cancer Immun 8 Suppl *1*: 1-4, 2008.
8 Banchereau J and Steinman RM: Dendritic cells and the control of immunity. Nature *392*: 245-252, 1998.
9 Mellman I and Steinman RM: Dendritic cells: specialized and regulated antigen processing machines. Cell *106*: 255-258, 2001.
10 Albert ML, Sauter B and Bhardwaj N: Dendritic cells acquire antigen from apoptotic cells and induce class I-restricted CTLs. Nature *392*: 86-89, 1998.
11 Liu WM, Dennis JL, Fowler DW and Dalgleish AG: The gene expression profile of unstimulated dendritic cells can be used as a predictor of function. Int J Cancer *130*: 979-990, 2011.
12 Kawabata R, Wada H, Isobe M, Saika T, Sato S, Uenaka A, Miyata H, Yasuda T, Doki Y, Noguchi Y, Kumon H, Tsuji K, Iwatsuki K, Shiku H, Ritter G, Murphy R, Hoffman E, Old LJ, Monden M and Nakayama E: Antibody response against NY-ESO-1 in CHP-NY-ESO-1 vaccinated patients. Int J Cancer *120*: 2178-2184, 2007.
13 Mizukami S, Kajiwara C, Ishikawa H, Katayama I, Yui K and Udono H: Both CD4+ and CD8+ T-cell epitopes fused to heat shock cognate protein 70 (hsc70) can function to eradicate tumors. Cancer Sci *99*: 1008-1015, 2008.
14 Udono H, Saito T, Ogawa M and Yui Y: Hsp-antigen fusion and their use for immunization. Methods *32*: 21-24, 2004.
15 Susumu S, Nagata Y, Ito S, Matsuo M, Valmori D, Yui K, Udono H and Kanematsu T: Cross-presentation of NY-ESO-1 cytotoxic T lymphocyte epitope fused to human heat shock cognate protein 70 by dendritic cells. Cancer Sci *99*: 107-112, 2008.
16 Udono H, Yamano T, Kawabata Y, Ueda M and Yui K: Generation of cytotoxic T lymphocytes by MHC class I ligands fused to heat-shock cognate protein 70. Int Immunol *13*: 1233-1242, 2001.
17 Gnjatic S, Nagata Y, Jager E, Stockert E, Shankara S, Roberts BL, Mazzara GP, Lee SY, Dunbar PR, Dupont B, Cerundolo V, Ritter G, Chen YT, Knuth A and Old LJ: Strategy for monitoring T-cell responses to NY-ESO-1 in patients with any HLA class I allele. Proc Natl Acad Sci USA *97*: 10917-10922, 2000.
18 Jager E, Chen YT, Drijfhout JW, Karbach J, Ringhoffer M, Jager D, Arand M, Wada H, Noguchi Y, Stockert E, Old LJ and Knuth A: Simultaneous humoral and cellular immune response against cancer-testis antigen NY-ESO-1: definition of human histocompatibility leukocyte antigen (HLA)-A2-binding peptide epitopes. J Exp Med *187*: 265-270, 1998.
19 Freudenthal PS and Steinman RM: The distinct surface of human blood dendritic cells, as observed after an improved isolation method. Proc Natl Acad Sci USA *87*: 7698-7702, 1990.
20 O'Doherty U, Steinman RM, Peng M, Cameron PU, Gezelter S, Kopeloff I, Swiggard WJ, Pope M and Bhardwaj N: Dendritic cells freshly isolated from human blood express CD4 and mature into typical immunostimulatory dendritic cells after culture in monocyte-conditioned medium. J Exp Med *178*: 1067-1076, 1993.
21 Chomarat P, Banchereau J, Davoust J and Palucka AK: IL-6 switches the differentiation of monocytes from dendritic cells to macrophages. Nat Immunol *1*: 510-514, 2000.
22 Gnjatic S, Atanackovic D, Jager E, Matsuo M, Selvakumar A, Altorki NK, Maki RG, Dupont B, Ritter G, Chen YT, Knuth A and Old LJ: Survey of naturally occurring CD4+ T cell responses against NY-ESO-1 in cancer patients: correlation with antibody responses. Proc Natl Acad Sci USA *100*: 8862-8867, 2003.
23 Fourie AM, Sambrook JF and Gething MJ: Common and divergent peptide binding specificities of hsp70 molecular chaperones. J Biol Chem *269*: 30470-30478, 1994.
24 Srivastava PK, Udono H, Blachere NE and Li Z: Heat shock proteins transfer peptides during antigen processing and CTL priming. Immunogenetics *39*: 93-98, 1994.
25 Suto R and Srivastava PK: A mechanism for the specific immunogenicity of heat shock protein-chaperoned peptides. Science *269*: 1585-1588, 1995.
26 Blachere NE, Li Z, Chandawarkar RY, Suto R, Jaikaria NS, Basu S, Udono H and Srivastava PK: Heat shock protein-peptide complexes, reconstituted *in vitro*, elicit peptide-specific cytotoxic T lymphocyte response and tumor immunity. J Exp Med *186*: 1315-1322, 1997.
27 Gong J, Zhang Y, Durfee J, Weng D, Liu C, Koido S, Song B, Apostolopoulos V and Calderwood SK: A heat shock protein 70-based vaccine with enhanced immunogenicity for clinical use. J Immunol *184*: 488-496, 2010.
28 Ohno S, Takano F, Ohta Y, Kyo S, Myojo S, Dohi S, Sugiyama H, Ohta T and Inoue M: Frequency of myeloid dendritic cells can predict the efficacy of Wilms' tumor 1 peptide vaccination. Anticancer Res *31*: 2447-2452, 2011.
29 Sallusto F and Lanzavecchia A: Efficient presentation of soluble antigen by cultured human dendritic cells is maintained by granulocyte/macrophage colony-stimulating factor plus interleukin 4 and downregulated by tumor necrosis factor alpha. J Exp Med *179*: 1109-1118, 1994.
30 Becker S, Warren MK and Haskill S: Colony-stimulating factor-induced monocyte survival and differentiation into macrophages in serum-free cultures. J Immunol *139*: 3703-3709, 1987.
31 Hikino H, Kasono K, Kanzaki M, Kai T, Konishi F and Kawakami M: Granulocyte/macrophage colony-stimulating factor and interleukin-4-induced dendritic cells. Anticancer Res *24*: 1609-1615, 2004.
32 Shinozaki Y, Wang S, Miyazaki Y, Miyazaki K, Yamada H, Yoshikai Y, Hara H and Yoshida H: Tumor-specific cytotoxic T cell generation and dendritic cell function are differentially regulated by interleukin 27 during development of anti-tumor immunity. Int J Cancer *124*: 1372-1378, 2009.
33 Ekkens MJ, Shedlock DJ, Jung E, Troy A, Pearce EL, Shen H and Pearce EJ: Th1 and Th2 cells help CD8 T-cell responses. Infect Immun *75*: 2291-2296, 2007.
34 Rissoan MC, Soumelis V, Kadowaki N, Grouard G, Briere F, de Waal Malefyt R and Liu YJ: Reciprocal control of T helper cell and dendritic cell differentiation. Science *283*: 1183-1186, 1999.
35 Sen D, Forrest L, Kepler TB, Parker I and Cahalan MD: Selective and site-specific mobilization of dermal dendritic cells and Langerhans cells by Th1- and Th2-polarizing adjuvants. Proc Natl Acad Sci USA *107*: 8334-8339, 2010.

36 Siegal FP, Kadowaki N, Shodell M, Fitzgerald-Bocarsly PA, Shah K, Ho S, Antonenko S and Liu YJ: The nature of the principal type 1 interferon-producing cells in human blood. Science *284*: 1835-1837, 1999.
37 Lebre MC and Tak PP: Dendritic cell subsets: their roles in rheumatoid arthritis. Acta Reumatol Port *33*: 35-45, 2008.
38 Liu YJ: Dendritic cell subsets and lineages, and their functions in innate and adaptive immunity. Cell *106*: 259-262, 2001.
39 Cernadas M, Lu J, Watts G and Brenner MB: CD1a expression defines an interleukin-12 producing population of human dendritic cells. Clin Exp Immunol *155*: 523-533, 2009.
40 Mohamadzadeh M, Berard F, Essert G, Chalouni C, Pulendran B, Davoust J, Bridges G, Palucka AK and Banchereau J: Interleukin 15 skews monocyte differentiation into dendritic cells with features of Langerhans cells. J Exp Med *194*: 1013-1020, 2001.
41 Wertel I, Bednarek W, Stachowicz N, Rogala E, Nowicka A and Kotarski J: Phenotype of dendritic cells generated from peripheral blood monocytes of patients with ovarian cancer. Transplant Proc *42*: 3301-3305, 2010.
42 Hildenbrand B, Lorenzen D, Sauer B, Hertkorn C, Freudenberg MA, Peters JH, Nesselhut T, Unger C and Azemar M: IFN-γ enhances T(H)1 polarisation of monocyte-derived dendritic cells matured with clinical-grade cytokines using serum-free conditions. Anticancer Res *28*: 1467-1476, 2008.
43 Mitani H, Katayama N, Araki H, Ohishi K, Kobayashi K, Suzuki H, Nishii K, Masuya M, Yasukawa K, Minami N and Shiku H: Activity of interleukin 6 in the differentiation of monocytes to macrophages and dendritic cells. Br J Haematol *109*: 288-295, 2000.

Received August 14, 2012
Revised October 9, 2012
Accepted October 10, 2012

World Journal of Gastroenterology

Online Submissions: http://www.wjgnet.com/1007-9327office
wjg@wjgnet.com
doi:10.3748/wjg.v18.i13.1470

World J Gastroenterol 2012 April 7; 18(13): 1470-1478
ISSN 1007-9327 (print) ISSN 2219-2840 (online)

ORIGINAL ARTICLE

Immunological milieu in the peritoneal cavity at laparotomy for gastric cancer

Akira Yoneda, Shinichiro Ito, Seiya Susumu, Mitsutoshi Matsuo, Ken Taniguchi, Yoshitsugu Tajima, Susumu Eguchi, Takashi Kanematsu, Yasuhiro Nagata

Akira Yoneda, Shinichiro Ito, Seiya Susumu, Ken Taniguchi, Yoshitsugu Tajima, Susumu Eguchi, Takashi Kanematsu, Department of Surgery, Nagasaki University Graduate School of Biomedical Sciences, Nagasaki 852-8051, Japan
Mitsutoshi Matsuo, Department of Surgery, Yamaguchi Prefectural Medical Center, Yamaguchi 747-8511, Japan
Yasuhiro Nagata, Department of Surgery, National Hospital Organization Nagasaki Medical Center, Nagasaki 856-8562, Japan
Author contributions: Yoneda A performed the majority of experiments; Ito S, Susumu S, Matsuo M, Taniguchi K, Tajima Y, Eguchi S were involved in editing the manuscript; Kanematsu T and Nagata Y designed the study and final approval of the version to be published.
Supported by Grant-in-Aid for Scientific Research (C), No. 22591459
Correspondence to: Akira Yoneda, MD, Department of Surgery, Nagasaki University Graduate School of Biomedical Sciences, 1-7-1 Sakamoto, Nagasaki 852-8501, Japan. dm06034e@cc.nagasaki-u.ac.jp
Telephone: +81-95-8197316 Fax: +81-95-8197319
Received: December 19, 2011 Revised: February 3, 2012
Accepted: February 16, 2012
Published online: April 7, 2012

Abstract

AIM: To investigate the immunological repertoire in the peritoneal cavity of gastric cancer patients.

METHODS: The peritoneal cavity is a compartment in which immunological host-tumor interactions can occur. However, the role of lymphocytes in the peritoneal cavity of gastric cancer patients is unclear. We observed 64 patients who underwent gastrectomy for gastric cancer and 11 patients who underwent laparoscopic cholecystectomy for gallstones and acted as controls. Lymphocytes isolated from both peripheral blood and peritoneal lavage were analyzed for surface markers of lymphocytes and their cytokine production by flow cytometry. $CD4^+CD25^{high}$ T cells isolated from the patient's peripheral blood were co-cultivated for 4 d with the intra-peritoneal lymphocytes, and a cytokine assay was performed.

RESULTS: At gastrectomy, $CCR7^-$ $CD45RA^-$ $CD8^+$ effector memory T cells were observed in the peritoneal cavity. The frequency of $CD4^+$ $CD25^{high}$ T cells in both the peripheral blood and peritoneal cavity was elevated in patients at advanced stage [control *vs* stage Ⅳ in the peripheral blood: 6.89 (3.39-10.4) *vs* 15.34 (11.37-19.31), $P < 0.05$, control *vs* stage Ⅳ in the peritoneal cavity: 8.65 (5.28-12.0) *vs* 19.56 (14.81-24.32), $P < 0.05$]. On the other hand, the suppression was restored with $CD4^+$ $CD25^{high}$ T cells from their own peripheral blood. This study is the first to analyze lymphocyte and cytokine production in the peritoneal cavity in patients with gastric cancer. Immune regulation at advanced stage is reversible at the point of gastrectomy.

CONCLUSION: The immunological milieu in the peritoneal cavity of patients with advanced gastric cancer elicited a Th2 response even at gastrectomy, but this response was reversible.

Key words: Cytokines; Gastric cancer; Lymphocytes; Peritoneal cavity; Regulatory T cell

Peer reviewer: Rasmus Goll, MD, Department of Gastroenterology, University Hospital of North Norway, Sykehusveien, Tromso 9038, Norway

Yoneda A, Ito S, Susumu S, Matsuo M, Taniguchi K, Tajima Y, Eguchi S, Kanematsu T, Nagata Y. Immunological milieu in the peritoneal cavity at laparotomy for gastric cancer. *World J Gastroenterol* 2012; 18(13): 1470-1478 Available from: URL: http://www.wjgnet.com/1007-9327/full/v18/i13/1470.htm DOI: http://dx.doi.org/10.3748/wjg.v18.i13.1470

INTRODUCTION

Tumor progression is governed not only by the genetic changes intrinsic to cancer cells, but also by epigenetic and environmental factors. Therefore, neoplastic cell factors and biophylactic side factors such as immune reactions are interacting in the survival and development of micrometastasis. Increasing evidence gleaned from studies in immune-compromised hosts suggests that the cellular mechanisms of immunosurveillance influence tumor development. There are several lines of research which indicate the critical role of the immune system in controlling the growth of malignant cells[1-5]. Thus, impairment of anti-tumor immunity, which leads to immunologic toleration of malignant cells, contributes to the development and progression of peritoneal metastasis[6]. The elimination phase of the cancer immunosurveillance mechanism is thought to be a continuous process, and local control of metastatic invasion by the immune system may be critical for survival. However, the role of lymphocytes in the peritoneal cavity for anti-tumor immunity in gastric cancer patients is unknown[7].

Studies in rodents have demonstrated that adoptive immunotherapy with antigen-specific $CD8^+$ T cells is effective for cancer, and there is evidence that this approach has therapeutic activity in humans[8-10]. Memory T cells circulate throughout all tissues of the body and are primed to rapidly produce secondary immune responses upon antigen challenge[11]. The nature of the cells that mediate the different facts of immunological memory remains unresolved. Natural killer T cells are a specialized subset of T cells. They express T-cell and natural killer-lineage cell surface markers and key cytokines, which regulate the course of the immune response. There are many mechanisms that regulate and dampen the immune response to cancers[12-15]. Regulatory T cells protect the host from autoimmune disease by suppressing self-reactive immune cells. As such, regulatory T cells may also block antitumor immune responses. Regulatory T cells have been an active research area in basic as well as in clinical immunology[16-18]. Th1 immune responses are considered to be essential for eradicating malignant cells. Based on the cytokine profile, interferon-gamma is a Th1 cytokine with an antitumor effect. Interleukin-10, a Th2 cytokine, inhibits Th1 immune responses and enhances the production of other Th2 cytokines[19-22].

In order to clarify the clinical significance of the host immune response within the peritoneal cavity in patients with gastric cancer, we conducted an immunological analysis of the peritoneal lavage obtained from patients at the time of gastrectomy.

MATERIALS AND METHODS

Patients

A total of 75 patients (50 males and 25 females; mean age: 64.3 years) were included in this study. Sixty-four patients were histologically diagnosed as having gastric cancer. Among these, 56 had gastrectomy, 2 underwent bypass operation, and 6 had exploratory laparotomy. Eleven patients who underwent laparoscopic cholecystectomy for benign disease acted as controls. The resected specimens were histologically examined by hematoxylin and eosin staining according to the general rules of the Japanese Classification of Gastric Carcinoma[23]. The investigation protocol was approved by the Institutional Review Board of the Nagasaki University School of Medicine (#14122694). Written informed consent was obtained from all patients. The stages of gastric cancer patients were as follows: stage I A, $n = 25$ patients; stage I B, $n = 13$; stage II, $n = 7$; stage III, $n = 7$; and stage IV, $n = 12$. The clinicopathological features of the patients are shown in Table 1.

Table 1 Clinicopathological features in the examined gastric cancer patients

Variables	No. of patients
Total cases	64
Age (yr)	67.5 ± 2.8
Sex (male/female)	42/22
Depth of tumor invasion	
T1	32
T2	20
T3	9
T4	3
Lymphnode metastasis	
N0	34
N1	12
N2	14
N3	4
Peritoneal metastasis	
Absent	56
Present	8
Cytology	
Negative	57
Positive	7
Stage	
Stage I A	25
Stage I B	13
Stage II	7
Stage III	7
Stage IV	12

Isolation of mononuclear cells from peripheral blood and peritoneal lavage

Endotracheal general anesthesia was induced and 10 mL of peripheral blood was taken from all patients. Four hundred milliliter of physiological saline was poured into the peritoneal cavity prior to manipulation of the tumor, and was recovered after being gently stirred. Half of the peritoneal lavage was allocated for conventional cytology and carcinoembryonic antigen (CEA) analysis by an enzyme-linked immunosorbent assay. The other half of the peritoneal lavage was immediately centrifuged at 2000 rpm for 10 min, and the supernatants were assayed for CEA values. The peritoneal CEA levels were then measured using an enzyme immunoassay kit (IMx-SERECT CEA, Dainabot, Tokyo) and the protein concentration was determined using a protein assay kit (Bio-Rad, Richmond, CA, United States). The cell component was used for lymphocyte analysis. Lymphocytes from peripheral

Table 2 Carcinoembryonic antigen values in sera and peritoneal lavage

Source	Control	Stage I A	Stage I B	Stage II	Stage III	Stage IV
CEA						
PB (ng/mL)	Not tested	2.09 (1.39-2.78)	2.03 (0.96-3.1)	3.06 (2.04-4.07)	2.54 (0.38-4.69)	7.98 (1.18-15.82)
PL (ng/g protein)	56.53 (21.82-91.24)	44.17 (27.37-60.96)	61.95 (11.98-111.91)	83.14 (7.31-187.54)	262.63 (7.26-517.26)	1234.00 (87.77-2380.22)
CD4/CD8						
PB (ratio)	5.379 (2.705-8.052)	5.595 (3.224-7.967)	4.571 (2.057-7.086)	5.277 (1.369-9.184)	7.999 (3.366-12.632)	4.156 (2.228-6.083)
PL (ratio)	0.494 (0.338-0.649)	0.553 (0.421-0.685)	0.697 (0.511-0.883)	0.638 (0.395-0.881)	1.242 (0.961-1.522)	1.158 (0.907-1.408)
CD45RA-/CCR7-						
PB (%)	60.43 (46.42-74.44)	58.29 (48.93-67.64)	53.92 (32.65-75.2)	57.36 (42.01-72.71)	49.01 (29.31-68.71)	45.73 (32.79-58.67)
PL (%)	81.17 (81.12-93.22)	81.67 (76.35-87.01)	76.2 (59.43-92.96)	72.3 (61.01-83.58)	68.36 (58.70-78.02)	51.92 (38.34-65.50)
NKT						
PB (%)	9.19 (5.83-12.54)	7.59 (5.63-9.56)	9.47 (4.41-14.53)	10.71 (1.55-19.87)	5.43 (0.54-10.33)	7.16 (3.95-10.3)
PL (%)	18.1 (9.83-26.37)	17.25 (13.54-20.97)	15.74 (9.23-22.25)	15.38 (7.71-23.04)	9.66 (1.2-18.11)	9.91 (6.94-12.88)

PB: Peripheral blood; PL: Peritoneal lavage; CI: Confidence interval. The data are presented as the median and 95% CI. The statistical analysis of the differences revealed higher CEA and CD4/CD8, lower $CD8^+$ effector memory T cells and NKT cells in the peritoneal cavity in patients with advanced stage than in controls.

blood were isolated by density centrifugation over Ficoll-Paque™ gradients (Amersham, Uppsala, Sweden).

Flow cytometry

The following monoclonal antibodies were used in the present study: fluorescein isothiocyanate (FITC)-conjugated anti-CD8, FITC-CD25, FITC-CD45RA, phycoerythrin (PE)-conjugated anti-CD4, PE-CD56, PE-CCR7, PE-IFN-γ, PE-IL-10, PE-Foxp3, cychrome (Cy)-conjugated anti-CD3, and Cy-CD8 (BD Pharmingen, San Diego, CA, United States). Single-cell suspensions were stained in phosphate-buffered saline-1% fetal calf serum at saturating concentrations according to standard procedures. Flow cytometry was performed on the BD Biosystems-FACSCanto II system (BD Biosciences, San Diego, CA, United States), and FACSDiva software (BD Biosciences, San Diego, CA, United States) was used for analysis. All analyses of T cells were carried out after gating by CD3. The ratio of the percentage of CD4 and CD8 cells was represented as the CD4/CD8 ratio.

Intracellular staining for Foxp3

Intracellular staining for Foxp3 was performed using the Human Foxp3 Buffer set (BD Pharmingen, San Diego, CA, United States) according to the manufacturer's protocol.

Cytokine assays

Anti-IFN-γ-PE and anti-IL-10-PE mAbs were used for the intracellular analysis of cytokine production. Peripheral and intra-peritoneal lymphocytes were activated with 10 ng/mL phorbol 12-myristate-13-acetate (PMA), 0.5 μg/mL Ionomycin, and 1 μL/mL GolgiPlug (BD Pharmingen, San Diego, CA, United States) for 4 h. Cells were washed, fixed and permeabilized by Cytofix/Cytoperm solution (BD Pharmingen, San Diego, CA, United States), and stained with titrated amounts of cytokine-specific antibodies.

Next, the $CD4^+$ $CD25^+$ T cells were isolated from peripheral blood by magnetic beads (Miltenyi Biotech,BergischGladbach, Germany). These $CD4^+$ $CD25^+$ T cells were mixed with intraperitoneal lymphocytes at a ratio of 1:10 and co-cultivated for 4 d in RPMI with 10% FBS. The $CD4^+$ $CD25^-$ T cells were co-cultivated with intraperitoneal lymphocytes as controls. The cytokine assay was performed by the intracellular cytokine method after 4 d of co-cultivation.

Statistical analysis

The statistical analysis was performed using the Kruskal-Wallis test (non-parametric ANOVA) using a personal computer and the StatViewV.5.0 software package (SAS Institute, Cary, NC, United States). *P* values less than 0.05 were considered to indicate statistical significance.

RESULTS

Carcinoembryonic antigen values in sera and peritoneal lavage

For the interaction between peripheral blood and the peritoneal cavity, we investigated the CEA values in both serum and peritoneal lavage at the time of surgery. The serum CEA values were elevated only in patients with stage IV disease. On the other hand, the values in peritoneal lavage were found to be elevated even at stage III, and they were also related to the clinical stage (Table 2).

Analysis of lymphocyte populations in peripheral blood and the peritoneal cavity

After purification of lymphocytes from peritoneal lavage, we investigated the phenotypes of lymphocytes in both peripheral blood and the peritoneal cavity. The mean value of the CD4/CD8 ratio for all patients was 2.17 in peripheral blood. The $CD8^+$ T cells were dominant in the peritoneal cavity and the CD4/CD8 ratio was reversed. The ratio in patients with stage III or IV was significantly higher than in stage I or control patients (Table 2).

The $CCR7^-$ $CD45RA^-$ $CD8^+$ T cells were counted as effector memory T cell subsets. The percentage of effector memory T cells in the peritoneal cavity was higher than that in peripheral blood. However, the percentage

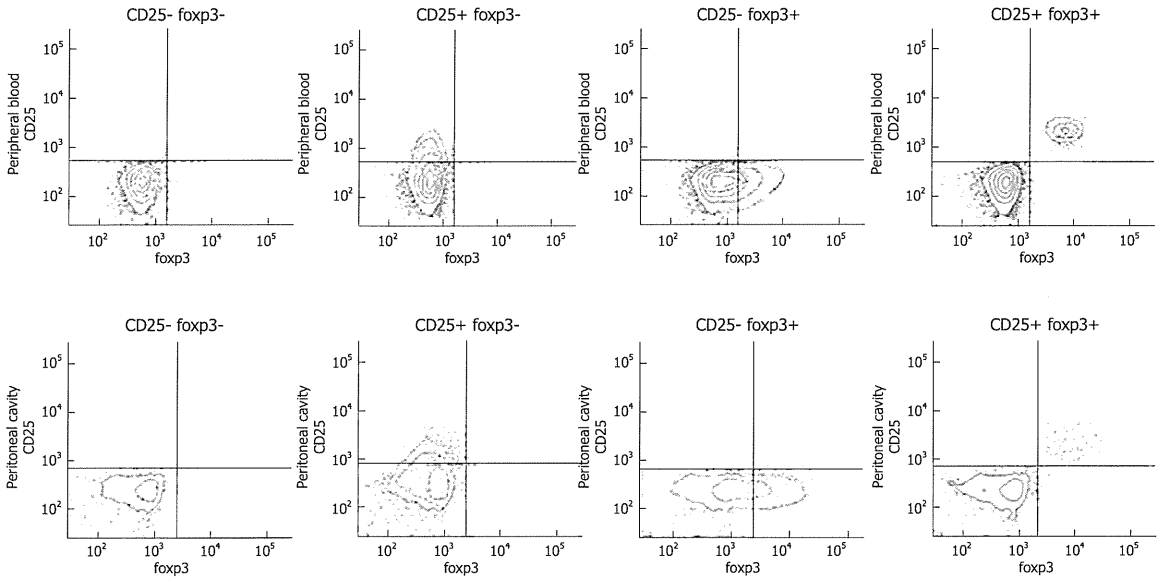

Figure 1 Co-staining with foxp3 and CD25 for CD4$^+$ T cells. High correlation was shown between both populations.

decreased in association with the clinical stage (Table 2). The CD3$^+$CD56$^+$ cells were measured as natural killer T cells. The percentage of these cells in the peritoneal lavage was also low in patients with stage Ⅲ or stage Ⅳ (Table 2). As the co-staining of foxp3 and CD25 revealed a high correlation between both populations, CD25^{high} was used following cytokine producing assays (Figure 1). The frequency of CD4$^+$ CD25^{high} T cells in patients with advanced stage cancer was higher than that in control patients in both peripheral blood and the peritoneal cavity (Figure 2A and B).

Cytokine production by lymphocytes

The cytokine production from CD3$^+$ T cells after stimulation with PMA + ionomycin was evaluated by a cytokine production assay. The lymphocytes in the peritoneal cavity were more sensitive for the production of IFN-γ than those in the peripheral blood. The ratio of IFN-γ producing cells in the peritoneal cavity was significantly lower in patients with advanced stage disease in comparison to the controls (Figure 3A and B). The ratio of IL-10 producing cells in the peritoneal cavity in patients with advanced stages was higher in comparison to the controls (Figure 3C and D).

Cytokine assays of intra-peritoneal lymphocytes after co-cultivation with self- CD4$^+$CD25^{high} T cells

In order to investigate whether the suppression of IFN-γ production from T cells in the peritoneal cavity at advanced stages was caused by CD4$^+$ CD25^{high} T cells, further assays were performed. The IFN-γ production of CD8$^+$ T cells was suppressed in intra-peritoneal lymphocytes co-cultivated with isolated CD4$^+$ CD25^{high} T cells from self-peripheral blood (Figure 4A). No inhibition was seen when the lymphocytes were co-cultivated with CD4$^+$ CD25$^-$ cells (Figure 4B).

DISCUSSION

The peritoneal cavity is a compartment in which the immunological host-tumor interaction can occur[24]. This study investigated lymphocytes in the peritoneal cavity of patients with gastric cancer in relation to anti-tumor immunity. Some tumors can acquire the ability to down-regulate immune responses and exploit this action to promote tumor cell proliferation, survival, and invasion[10,25]. Therefore, the presence of leukocytes in the peritoneal cavity may be a consequence of an immune response that favors either dissemination of tumor cells or a protective host response. Malignant ascites has been used as a common source of immunological analysis in previous reports[11,26]. To the best of our knowledge, there are no reports describing the lymphocyte and cytokine production ability in peritoneal lavage from patients with gastric cancer at the time of gastrectomy.

In our initial experiments, the CEA values in peritoneal lavage were found to correlate with the clinical stages. Interestingly, the CEA values were elevated even in cases without serosal invasion. This result suggests that some fragments of cancer cells may spread throughout the peritoneal cavity and induce an immune reaction between the tumor and host[26,27].

The frequency of CD4$^+$ T cells in all patients was higher than that of CD8$^+$ T cells in peripheral blood, but this pattern was reversed in peritoneal lavage fluid. CD8$^+$ T cells were dominant in the peritoneal cavity. Our data suggested that the immunological environment in the peripheral blood is different from that in the peritoneal cavity. There were significant differences in the CD4/CD8 ratio in the peritoneal cavity between gastric cancer

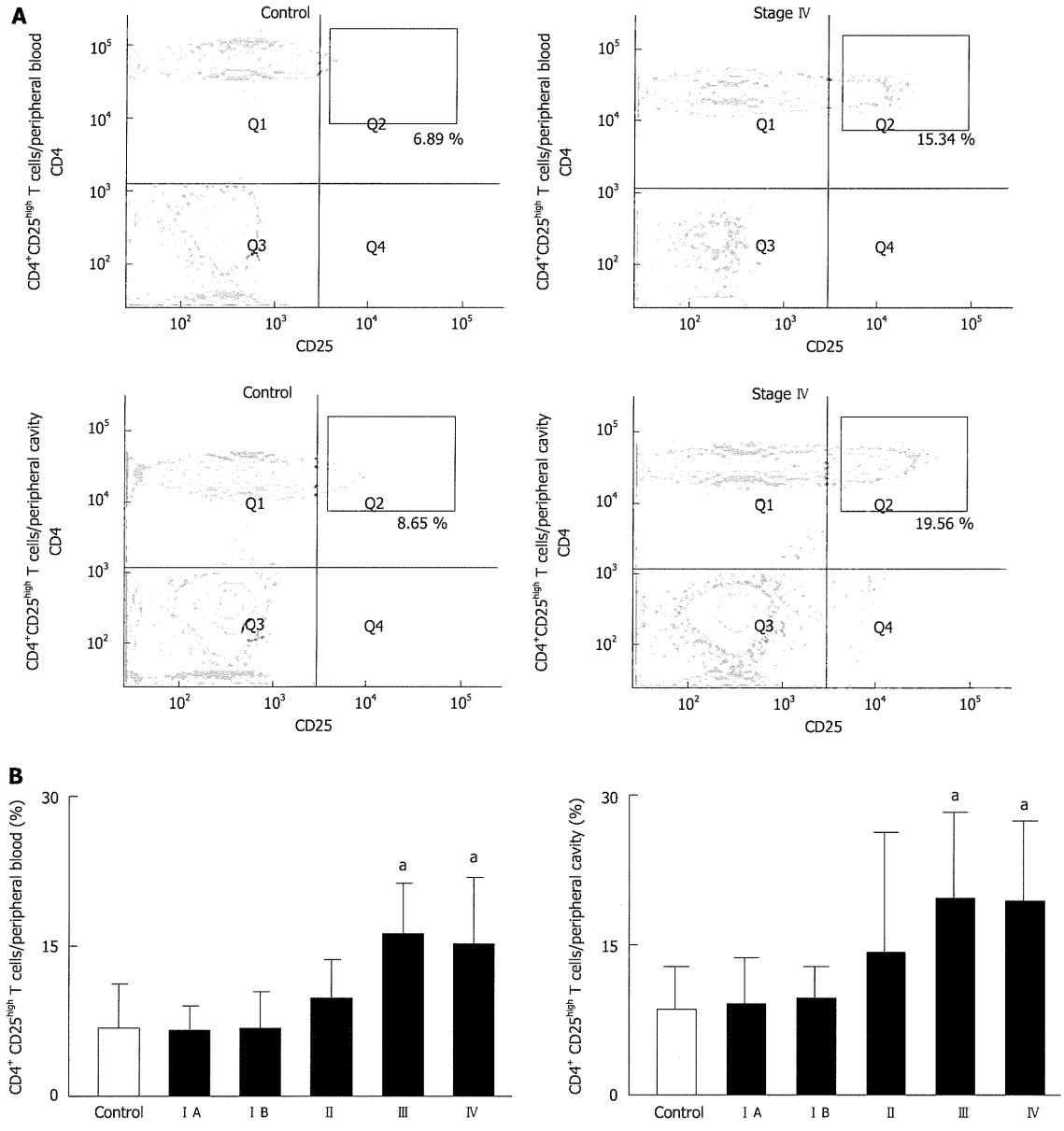

Figure 2 Analysis of lymphocyte populations in peripheral blood and the peritoneal cavity. A: The gating and counting of $CD4^+$ $CD25^{high}$ T cell population by flow cytometry; B: The percentage of $CD4^+$ $CD25^{high}$ T cells in the $CD4^+$ T cell population in peripheral blood and peritoneal lavage of patients at each stage of gastric cancer and control patients. Data are presented as the mean ± SD.

patients at advanced stage and control patients. Cancer progression may have an effect on the balance of the T cell population in the peritoneal cavity.

Immunological memory is demonstrated by following T cell subsets: lymph-node-homing cells lacking inflammatory and cytotoxic function (defined as central memory T cells, $CCR7^+$ $CD45RA^-$) and tissue-homing cells endowed with various effector functions (defined as effector memory T cells, $CCR7^-$ $CD45RA^-$). These two subsets allow for the division of labor among memory cells. Effector memory T cells represent a readily available pool of antigen-primed cells that can enter peripheral tissues to mediate inflammatory reactions or cytotoxicity, thus rapidly containing invasive pathogens and cancer antigens[11,28-31]. Our data show that $CD8^+$ effector memory T cells were rich in the peritoneal cavity. This indicates the migration of effector memory cells from the peripheral blood to local sites. However, in advanced cases, the frequency of $CD8^+$ effector memory cells in the peritoneal lavage was low. These results suggest that the peritoneal cavity exerts the local immune response, more than peripheral blood.

Natural killer T cells, a unique lymphocyte subpopulation, are characterized by the expression of invariant an-

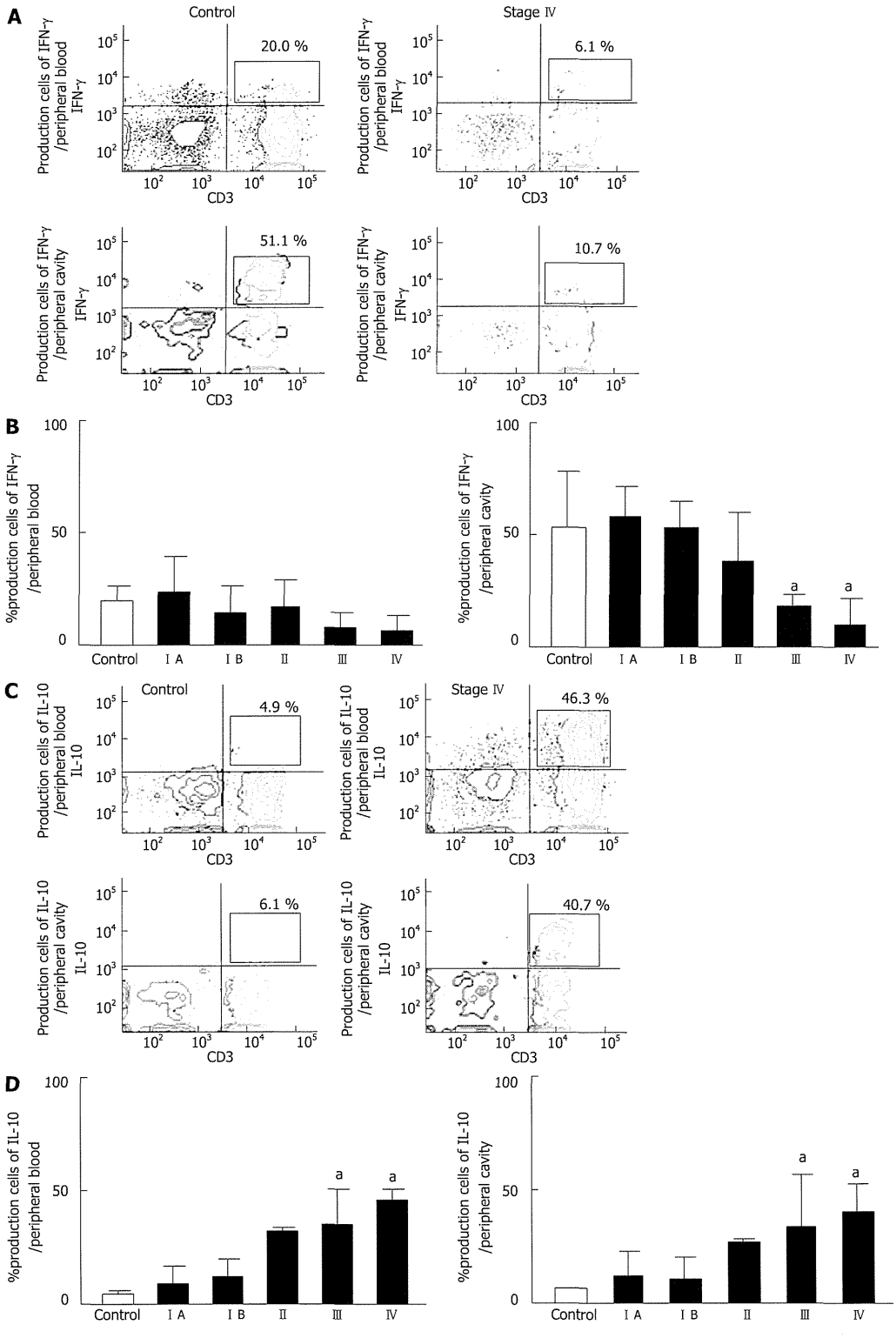

Figure 3 Cytokine production by lymphocytes. A: The gating and counting of the IFN-γ producing cell population by flow cytometry; B: The percentage of IFN-γ producing cells in the $CD3^+$ cell population stimulated with PMA + ionomycin in peripheral blood and peritoneal lavage of patients at each stage of gastric cancer and control patients Data are presented as the mean ± SD. The statistical analysis was performed by the Kruskal-Wallis test. After gating of CD3+ T cells, 10 000 events were analyzed. The production of IFN-γ in the peritoneal cavity was higher than that in the peripheral blood. The ratio of IFN-γ production cells in the peritoneal lavage was significantly lower in patients with advanced-stage than in controls [control *vs* stage Ⅳ: 51.1 (35.1-67.1) *vs* 10.7 (2.6-22.1), $^aP < 0.05$]; C: The gating and counting of the IL-10 producing cell population by flow cytometry; D: The percentage of IL-10 producing cells in the $CD3^+$ cells stimulated with PMA + ionomycin in peripheral blood and peritoneal lavage of patients at each stage of gastric cancer and control patients. Data are presented as the mean ± SD. The ratio of IL-10 producing cells in peripheral blood and intra-peritoneal lymphocytes was significantly higher in patients at advanced stage than in controls [control *vs* stage Ⅳ: 6.1 (3.94-8.25) *vs* 40.7 (18.35-63.0), $^aP < 0.05$].

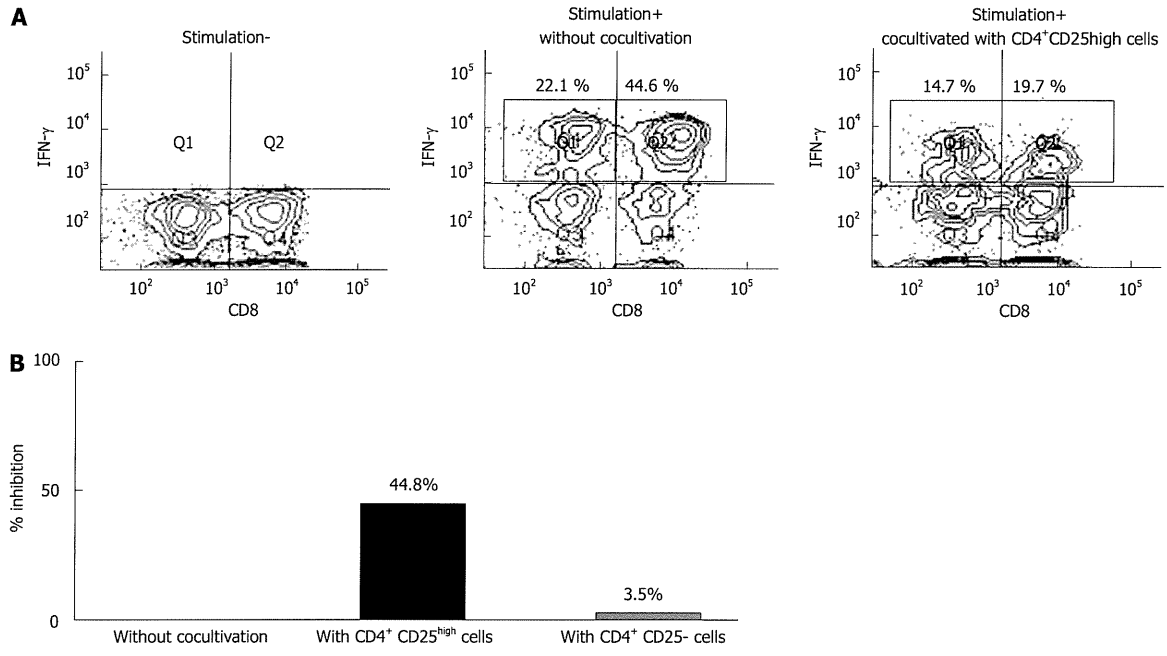

Figure 4 Cytokine assays of intra-peritoneal lymphocytes after co-cultivation with self-CD4$^+$CD25^{high}T cells. A: IFN-γ production in intra-peritoneal lymphocytes co-cultivated with self- CD4$^+$ CD25^{high} T cells; B: Either CD4$^+$ CD25^{high} T cells or CD4$^+$ CD25$^-$ T cells.

tigen receptors[12,13]. Natural killer T cells have been suggested to serve as a bridge between innate and acquired immunity[14,15]. However, the mechanisms underlying the anti-tumor effect of human natural killer T cell-mediated immunotherapy remain unclear so far. The frequency of natural killer T cells was lower in patients with stages Ⅲ and Ⅳ than in control patients. Therefore, a decrease in the number of natural killer T cells in the peritoneal cavity may be one aspect of the interaction between host-immunity and cancer progression.

Recent studies have shown that CD4$^+$ CD25^{high} foxp3$^+$ T cells exhibiting regulatory/suppressive properties are naturally present in humans[16-18]. The roles of regulatory T cells have been active topics of research in both basic and clinical immunology. Naturally-occurring regulatory T cells represent a small fraction (5%-6%) of the overall CD4$^+$ T cell population, and play an important role in down-regulation of the response of T cells to foreign and self antigens[31]. The depletion of this subset of regulatory T cells in normal hosts results in various autoimmune diseases because the host immune system is unchecked and attacks the body's own tissues[28]. Despite the importance of these cells in preventing autoimmune disease, their presence in the tumor microenvironment diminishes anti-tumor immune responses[32-36].

Within the CD4$^+$ T cell subset, there is a population of naturally occurring foxp3$^+$ T cells that are defined as regulatory T cells. These cells can be identified as CD4$^+$foxp3$^+$ T cells by flow cytometry. However, because foxp3 is intracellular and requires permeabilization of cells for detection by flow cytometry, regulatory T cells are isolated as CD4$^+$CD25^{high} T cells, which were shown to have functional suppressive abilities in our co-culture experiments[37]. In the present study, the mean percentage of CD4$^+$ CD25^{high} T cells in the peritoneal cavity in advanced gastric cancer patients was higher than that of control patients. After the co-cultivation of the self-CD4$^+$ CD25^{high} T cell population of intra-peritoneal lymphocytes, the production of IFN-γ was inhibited.

IFN-γ, a Th1 cytokine, not only exerts an anti-tumor effect, but also inhibits the proliferation of Th2 clones[19-20]. IL-10, a Th2 cytokine, suppresses the synthesis of Th1 cytokines such as IFN-γ[21-22]. This study showed that the production of intracellular cytokines in the peritoneal cavity was higher than that in the peripheral blood after appropriate stimulation. IFN-γ production was down-regulated in advanced cases, but not in the controls and stage I patients. On the other hand, IL-10 production was up-regulated, which revealed the switch of Th1 and Th2 responses in the peritoneal cavity of these patients. IFN-γ production in intra-peritoneal lymphocytes was suppressed after co-cultivation with self-CD4$^+$ CD25^{high} T cells, but not CD4$^+$ CD25$^-$ T cells. Interestingly, the replacement of CD4$^+$ CD25$^-$ T cells for CD4$^+$ CD25^{high} T cells could recover the production of IFN-γ in intra-peritoneal lymphocytes.

COMMENTS

Background

The peritoneal cavity is a compartment in which immunological host-tumor interactions can occur. Neoplastic cell factors and biophylactic side factors such as immune reactions are interacting in the survival and development of micro-metastasis. However, the role of lymphocytes in the peritoneal cavity of gastric cancer patients is unclear.

Research frontiers

Clinical and experimental studies have established that leukocyte infiltrations around tumors promote the development or regression of solid tumors, but-whether the organ-specific cellular and molecular programs promote tumor growth or exhibit anti-tumor immunity by leukocytes are incompletely understood. Recent studies have shown that $CD4^+$ $CD25^{high}$ $foxp3^+$ T cells exhibiting regulatory/suppressive properties are naturally present in humans. The roles of regulatory T cells have been active topics of research in both basic and clinical immunology.

Innovations and breakthroughs

In most previous studies, malignant ascites have been a common source of immunological analysis. However, there are no reports describing the lymphocyte and cytokine production ability in peritoneal lavage from patients with gastric cancer at the time of gastrectomy. In the present study, $CD4^+$ $CD25^{high}$ T cells were found to be increased in the peritoneal cavity of advanced gastric cancer patients, but in the co-cultivation of the self- $CD4^+$ $CD25^{high}$ T cell population of intra-peritoneal lymphocytes, the production of IFN-γwas inhibited.

Applications

Peritoneal lavage samples from patients with gastric cancer are more susceptible than peripheral blood for monitoring the interaction between the host's immune system and tumor cells.

Terminology

Regulatory T cells: Regulatory T cells contribute to the maintenance of immunologic self-tolerance. Recent reports underscore that regulatory T cells not only play a role in the maintenance of immunotolerance but are also potent inhibitors of antitumor immune responses.

Peer review

The authors have investigated T-cells isolated from peripheral blood and peritoneal lavage in patients with gastric cancer and controls. Main findings are that in stage Ⅲ and Ⅳ gastric cancers the lavage fluid contains less CD8 memory cells, NKT cells and more $CD25^{high}$ regulatory T cells.

REFERENCES

1 **Huber V**, Fais S, Iero M, Lugini L, Canese P, Squarcina P, Zaccheddu A, Colone M, Arancia G, Gentile M, Seregni E, Valenti R, Ballabio G, Belli F, Leo E, Parmiani G, Rivoltini L. Human colorectal cancer cells induce T-cell death through release of proapoptotic microvesicles: role in immune escape. *Gastroenterology* 2005; **128**: 1796-1804

2 **Galon J**, Costes A, Sanchez-Cabo F, Kirilovsky A, Mlecnik B, Lagorce-Pagès C, Tosolini M, Camus M, Berger A, Wind P, Zinzindohoué F, Bruneval P, Cugnenc PH, Trajanoski Z, Fridman WH, Pagès F. Type, density, and location of immune cells within human colorectal tumors predict clinical outcome. *Science* 2006; **313**: 1960-1964

3 **Susumu S**, Nagata Y, Ito S, Matsuo M, Valmori D, Yui K, Udono H, Kanematsu T. Cross-presentation of NY-ESO-1 cytotoxic T lymphocyte epitope fused to human heat shock cognate protein 70 by dendritic cells. *Cancer Sci* 2008; **99**: 107-112

4 **Koizumi K**, Hojo S, Akashi T, Yasumoto K, Saiki I. Chemokine receptors in cancer metastasis and cancer cell-derived chemokines in host immune response. *Cancer Sci* 2007; **98**: 1652-1658

5 **Tsujimoto H**, Ono S, Ichikura T, Matsumoto Y, Yamamoto J, Hase K. Roles of inflammatory cytokines in the progression of gastric cancer: friends or foes? *Gastric Cancer* 2010; **13**: 212-221

6 **Nan KJ**, Wei YC, Zhou FL, Li CL, Sui CG, Hui LY, Gao CG. Effects of depression on parameters of cell-mediated immunity in patients with digestive tract cancers. *World J Gastroenterol* 2004; **10**: 268-272

7 **Atanackovic D**, Block A, de Weerth A, Faltz C, Hossfeld DK, Hegewisch-Becker S. Characterization of effusion-infiltrating T cells: benign versus malignant effusions. *Clin Cancer Res* 2004; **10**: 2600-2608

8 **Cheever MA**, Greenberg PD, Fefer A. Specificity of adoptive chemoimmunotherapy of established syngeneic tumors. *J Immunol* 1980; **125**: 711-714

9 **Dudley ME**, Wunderlich JR, Robbins PF, Yang JC, Hwu P, Schwartzentruber DJ, Topalian SL, Sherry R, Restifo NP, Hubicki AM, Robinson MR, Raffeld M, Duray P, Seipp CA, Rogers-Freezer L, Morton KE, Mavroukakis SA, White DE, Rosenberg SA. Cancer regression and autoimmunity in patients after clonal repopulation with antitumor lymphocytes. *Science* 2002; **298**: 850-854

10 **Dudley ME**, Wunderlich JR, Yang JC, Sherry RM, Topalian SL, Restifo NP, Royal RE, Kammula U, White DE, Mavroukakis SA, Rogers LJ, Gracia GJ, Jones SA, Mangiameli DP, Pelletier MM, Gea-Banacloche J, Robinson MR, Berman DM, Filie AC, Abati A, Rosenberg SA. Adoptive cell transfer therapy following non-myeloablative but lymphodepleting chemotherapy for the treatment of patients with refractory metastatic melanoma. *J Clin Oncol* 2005; **23**: 2346-2357

11 **Sallusto F**, Lenig D, Förster R, Lipp M, Lanzavecchia A. Two subsets of memory T lymphocytes with distinct homing potentials and effector functions. *Nature* 1999; **401**: 708-712

12 **Taniguchi M**, Harada M, Kojo S, Nakayama T, Wakao H. The regulatory role of Valpha14 NKT cells in innate and acquired immune response. *Annu Rev Immunol* 2003; **21**: 483-513

13 **Brigl M**, Brenner MB. CD1: antigen presentation and T cell function. *Annu Rev Immunol* 2004; **22**: 817-890

14 **Taniguchi M**, Seino K, Nakayama T. The NKT cell system: bridging innate and acquired immunity. *Nat Immunol* 2003; **4**: 1164-1165

15 **Motohashi S**, Nakayama T. Clinical applications of natural killer T cell-based immunotherapy for cancer. *Cancer Sci* 2008; **99**: 638-645

16 **Sakaguchi S**. Naturally arising CD4+ regulatory t cells for immunologic self-tolerance and negative control of immune responses. *Annu Rev Immunol* 2004; **22**: 531-562

17 **Linehan DC**, Goedegebuure PS. CD25+ CD4+ regulatory T-cells in cancer. *Immunol Res* 2005; **32**: 155-168

18 **Imai H**, Saio M, Nonaka K, Suwa T, Umemura N, Ouyang GF, Nakagawa J, Tomita H, Osada S, Sugiyama Y, Adachi Y, Takami T. Depletion of CD4+CD25+ regulatory T cells enhances interleukin-2-induced antitumor immunity in a mouse model of colon adenocarcinoma. *Cancer Sci* 2007; **98**: 416-423

19 **Fernandez-Botran R**, Sanders VM, Mosmann TR, Vitetta ES. Lymphokine-mediated regulation of the proliferative response of clones of T helper 1 and T helper 2 cells. *J Exp Med* 1988; **168**: 543-558

20 **Rayman P**, Wesa AK, Richmond AL, Das T, Biswas K, Raval G, Storkus WJ, Tannenbaum C, Novick A, Bukowski R, Finke J. Effect of renal cell carcinomas on the development of type 1 T-cell responses. *Clin Cancer Res* 2004; **10**: 6360S-6366S

21 **Fiorentino DF**, Zlotnik A, Vieira P, Mosmann TR, Howard M, Moore KW, O'Garra A. IL-10 acts on the antigen-presenting cell to inhibit cytokine production by Th1 cells. *J Immunol* 1991; **146**: 3444-3451

22 **Bai XF**, Zhu J, Zhang GX, Kaponides G, Höjeberg B, van der Meide PH, Link H. IL-10 suppresses experimental autoimmune neuritis and down-regulates TH1-type immune responses. *Clin Immunol Immunopathol* 1997; **83**: 117-126

23 **Japanese Gastric Cancer Association.** Japanese classification of gastric carcinoma--2nd English edition--response assessment of chemotherapy and radiotherapy for gastric carcinoma: clinical criteria. *Gastric Cancer* 2001; **4**: 1-8

24 **Olszewski WL**, Kubicka U, Tarnowski W, Bielecki K, Ziolkowska A, Wesolowska A. Activation of human peritoneal immune cells in early stages of gastric and colon cancer. *Surgery* 2007; **141**: 212-221

25 **Mori T**, Shimizu M, Iwaguchi T. Immunological characterization and clinical significance of low mobility cells appearing in the peripheral blood mononuclear cells of cancer patients. *Eur J Cancer Clin Oncol* 1988; **24**: 1463-1469

26 **Marutsuka T**, Shimada S, Shiomori K, Hayashi N, Yagi Y, Yamane T, Ogawa M. Mechanisms of peritoneal metastasis after operation for non-serosa-invasive gastric carcinoma: an ultrarapid detection system for intraperitoneal free cancer cells and a prophylactic strategy for peritoneal metastasis. *Clin Cancer Res* 2003; **9**: 678-685

27 **Jung M**, Jeung HC, Lee SS, Park JY, Hong S, Lee SH, Noh SH, Chung HC, Rha SY. The clinical significance of ascitic fluid CEA in advanced gastric cancer with ascites. *J Cancer Res Clin Oncol* 2010; **136**: 517-526

28 **Sallusto F**, Geginat J, Lanzavecchia A. Central memory and effector memory T cell subsets: function, generation, and maintenance. *Annu Rev Immunol* 2004; **22**: 745-763

29 **Berger C**, Jensen MC, Lansdorp PM, Gough M, Elliott C, Riddell SR. Adoptive transfer of effector CD8+ T cells derived from central memory cells establishes persistent T cell memory in primates. *J Clin Invest* 2008; **118**: 294-305

30 **Ye SW**, Wang Y, Valmori D, Ayyoub M, Han Y, Xu XL, Zhao AL, Qu L, Gnjatic S, Ritter G, Old LJ, Gu J. Ex-vivo analysis of CD8+ T cells infiltrating colorectal tumors identifies a major effector-memory subset with low perforin content. *J Clin Immunol* 2006; **26**: 447-456

31 **Wang HY**, Wang RF. Regulatory T cells and cancer. *Curr Opin Immunol* 2007; **19**: 217-223

32 **Nishikawa H**, Kato T, Hirayama M, Orito Y, Sato E, Harada N, Gnjatic S, Old LJ, Shiku H. Regulatory T cell-resistant CD8+ T cells induced by glucocorticoid-induced tumor necrosis factor receptor signaling. *Cancer Res* 2008; **68**: 5948-5954

33 **Curiel TJ**, Coukos G, Zou L, Alvarez X, Cheng P, Mottram P, Evdemon-Hogan M, Conejo-Garcia JR, Zhang L, Burow M, Zhu Y, Wei S, Kryczek I, Daniel B, Gordon A, Myers L, Lackner A, Disis ML, Knutson KL, Chen L, Zou W. Specific recruitment of regulatory T cells in ovarian carcinoma fosters immune privilege and predicts reduced survival. *Nat Med* 2004; **10**: 942-949

34 **Wing K**, Onishi Y, Prieto-Martin P, Yamaguchi T, Miyara M, Fehervari Z, Nomura T, Sakaguchi S. CTLA-4 control over Foxp3+ regulatory T cell function. *Science* 2008; **322**: 271-275

35 **Onishi Y**, Fehervari Z, Yamaguchi T, Sakaguchi S. Foxp3+ natural regulatory T cells preferentially form aggregates on dendritic cells in vitro and actively inhibit their maturation. *Proc Natl Acad Sci USA* 2008; **105**: 10113-10118

36 **Stanzer S**, Dandachi N, Balic M, Resel M, Samonigg H, Bauernhofer T. Resistance to apoptosis and expansion of regulatory T cells in relation to the detection of circulating tumor cells in patients with metastatic epithelial cancer. *J Clin Immunol* 2008; **28**: 107-114

37 **Gnjatic S**, Altorki NK, Tang DN, Tu SM, Kundra V, Ritter G, Old LJ, Logothetis CJ, Sharma P. NY-ESO-1 DNA vaccine induces T-cell responses that are suppressed by regulatory T cells. *Clin Cancer Res* 2009; **15**: 2130-2139

S- Editor Gou SX **L- Editor** Webster JR **E- Editor** Zhang DN

Nucleic Acids Research Advance Access published May 31, 2012

Nucleic Acids Research, 2012, 1–15
doi:10.1093/nar/gks506

LRPPRC/SLIRP suppresses PNPase-mediated mRNA decay and promotes polyadenylation in human mitochondria

Takeshi Chujo[1], Takayuki Ohira[1], Yuriko Sakaguchi[1], Naoki Goshima[2], Nobuo Nomura[2,3], Asuteka Nagao[1] and Tsutomu Suzuki[1,*]

[1]Department of Chemistry and Biotechnology, Graduate School of Engineering, University of Tokyo, Tokyo, 7-3-1 Hongo, Bunkyo-ku, Tokyo 113-8656, [2]National Institute of Advanced Industrial Science and Technology, 2-42 Aomi, Koto-ku, Tokyo 135-0064 and [3]Faculty of Human Studies, Musashino University, 1-1-20 Shinmachi, Nishitokyo, Tokyo 202-8585, Japan

Received February 26, 2012; Revised April 17, 2012; Accepted May 8, 2012

ABSTRACT

In human mitochondria, 10 mRNAs species are generated from a long polycistronic precursor that is transcribed from the heavy chain of mitochondrial DNA, in theory yielding equal copy numbers of mRNA molecules. However, the steady-state levels of these mRNAs differ substantially. Through absolute quantification of mRNAs in HeLa cells, we show that the copy numbers of all mitochondrial mRNA species range from 6000 to 51 000 molecules per cell, indicating that mitochondria actively regulate mRNA metabolism. In addition, the copy numbers of mitochondrial mRNAs correlated with their cellular half-life. Previously, mRNAs with longer half-lives were shown to be stabilized by the LRPPRC/SLIRP complex, which we find that cotranscriptionally binds to coding sequences of mRNAs. We observed that the LRPPRC/SLIRP complex suppressed 3′ exonucleolytic mRNA degradation mediated by PNPase and SUV3. Moreover, LRPPRC promoted the polyadenylation of mRNAs mediated by mitochondrial poly(A) polymerase (MTPAP) *in vitro*. These findings provide a framework for understanding the molecular mechanism of mRNA metabolism in human mitochondria.

INTRODUCTION

Human mitochondria contain circular, double-stranded DNAs (mtDNA) of 16.6 kb, which encode 37 genes in both the H- and L-strands: 13 of these encode the essential subunits of the respiratory complexes I, III, IV and V; 22 encode tRNAs and 2 encode rRNAs (1) (Figure 1A). To translate the 13 genes that encode proteins, mitochondria have a specific protein synthesis machinery in which all tRNAs and rRNAs are supplied from mtDNA. A long polycistronic precursor RNA of the H-strand is transcribed from the H-strand promoter 2 (HSP2) (Figure 1A) and is then processed to yield 10 mRNAs for 12 genes (*ND4L/4* and *ATP8/6* are bicistronic), 2 rRNAs and 14 tRNAs (2). Only the mRNA for *ND6* is transcribed from the L-strand of mtDNA, together with eight tRNAs (Figure 1A). Hence, in theory, equal copy numbers of 10 mRNA species are generated stoichiometrically from the single polycistronic transcript of the H-strand. However, the steady-state levels of these 10 mRNAs have been reported to differ substantially (3,4). In addition, our group previously determined that the half-life of each mitochondrial mRNA in HeLa cells ranged from 68 to 231 min (5). These studies implied the existence of a post-transcriptional regulatory mechanism that controls the stability and metabolism of mRNAs in mitochondria.

Leigh Syndrome French Canadian variant (LSFC) is an autosomal, neurodegenerative disease from which patients die of fulminant metabolic acidosis (6). LSFC is characterized by a tissue-specific deficiency in complex IV (cytochrome c oxidase) activity, which particularly affects the brain and liver (7). The cause of LSFC was identified as a C-to-T point mutation at nucleotide position 1119 of the leucine-rich pentatricopeptide repeat (PPR) motif-containing protein (*LRPPRC*) gene (8). This mutation changes the alanine at position 354 to valine (A354V), and the cellular level of mutant LRPPRC is reduced significantly (9). Moreover, the steady-state levels of mitochondrial mRNAs are also significantly decreased (9,10). LRPPRC is predominantly localized to mitochondria (11).

*To whom correspondence should be addressed. Tel: +81 3 5841 8752; Fax: +81 3 5841 0550; Email: ts@chembio.t.u-tokyo.ac.jp

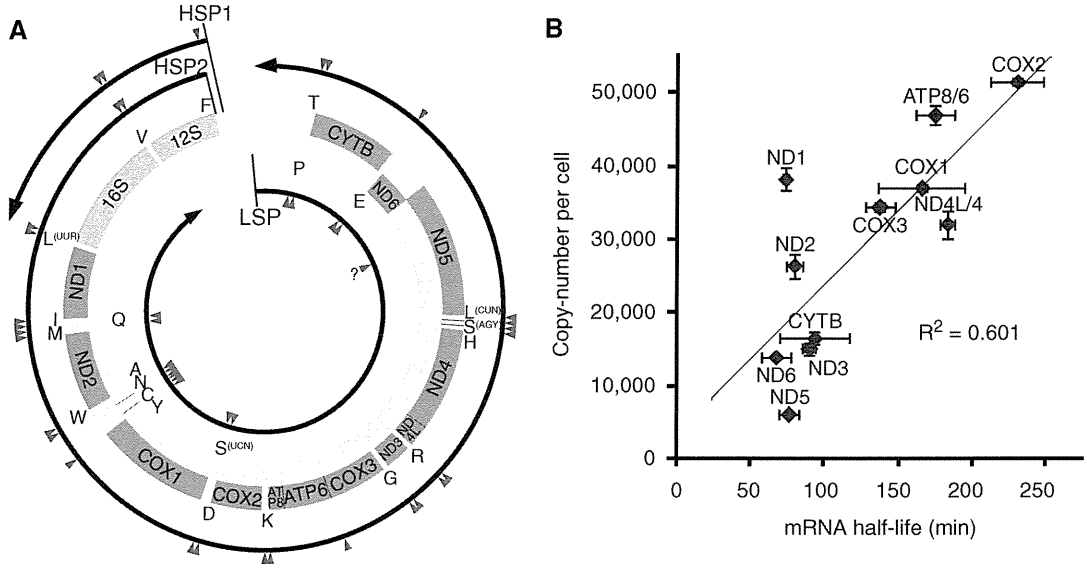

Figure 1. Variable steady-state levels and half-lives of human mitochondrial mRNAs. (**A**) Schematic representation of human mtDNA with its gene organization and transcriptional units. The outer and inner circles represent the H- and L-strands of mtDNA, respectively. Protein (blue) and ribosomal RNA (orange) genes are interspersed with 22 tRNA genes (yellow, with single-letter amino acid codes). The L- and H-strand transcripts from the promoters LSP, HSP1 and HSP2 are indicated by circular arrows showing the direction of transcription. The sites for RNA processing are indicated by arrowheads. The processing site for *ND6* is shown as a question mark because its 3′-end has not yet been defined (4,18). (**B**) Copy numbers of mRNAs (means ± SD, $n = 3$) in HeLa cells plotted against their half-lives in HeLa cells, as previously reported (5). The correlation factor (R^2) of the plot is 0.601.

LRPPRC contains 16 PPR motifs (12), which are predicted to bind to single-stranded nucleic acids (13). In fact, LRPPRC can bind to a single-stranded RNA *in vitro* and is found crosslinked to poly(A)$^+$ RNA in mitochondrial fractions isolated from ultraviolet-irradiated cells (11). LRPPRC physically forms a stable complex with the SRA stem-loop-interacting RNA-binding protein (SLIRP) (9), which is a small protein bearing a single RNA recognition motif (RRM) that is localized primarily to mitochondria (14). Knockdown of either *LRPPRC* (15) or *SLIRP* (16) results in similar decreases in mRNA levels but does not affect the levels of tRNAs or rRNAs, indicating that the LRPPRC/SLIRP complex plays a specific role in mRNA maturation or stabilization after transcription in mitochondria (9). In addition, a *LRPPRC* knockout mouse is embryonic lethal and deficient in mRNA polyadenylation (17). Moreover, an aberrant pattern of mitochondrial translation was observed in a *LRPPRC* knockout mouse, demonstrating that LRPPRC is necessary for regulated translation in mammalian mitochondria.

Human mitochondrial mRNAs have short (~50 nt) poly(A) tails (18), whose lengths are regulated by mitochondria-specific poly(A) polymerase (MTPAP) (19,20) and polynucleotide phosphorylase (PNPase) (19). The role of the poly(A) tail in mRNA stabilization or destabilization remains elusive. When *MTPAP* was knocked down by RNAi, the poly(A) tail of each mRNA was shortened and the steady-state levels of several mRNAs, including *COX1* and *COX2*, were reduced, while mRNA levels for *ND1*, *ND2*, *ND3* and *CYTB* were unchanged or increased (5,19,20). When artificial deadenylation of mt mRNAs was induced by targeting cytosolic deadenylase (PARN) to mitochondria (21) or by overexpressing *PDE12* (22), the steady-state level of *COX1* and *COX2* mRNAs decreased, while mRNA levels of *ND1*, *ND2*, *ND3* and *CYTB* increased.

The entity of the mRNA degradation machinery in human mitochondria has remained elusive (23). PNPase is one of the major 3′–5′ exonucleases in bacteria (24). In human mitochondria, the involvement of PNPase in homeostasis of the poly(A) tail has been suggested. Downregulation of *PNPase* by RNAi resulted in the elongation of mRNA poly(A) tails for *COX1*, *COX2*, *COX3*, *ATP8/6* and *ND3* (19), although the steady-state levels of these mRNAs and proteins were unaffected (19,25). This indicated that PNPase participates in the deadenylation of the poly(A) tail of a subset of mRNAs. However, PNPase mainly localizes to the intermembrane space (IMS) of mitochondria where mRNAs are absent (25). In addition, PNPase is involved in the transport of the RNA component for RNaseMRP into mitochondria (26) and participates in the degradation of *c-myc* mRNA (27) and miR-221 in human melanoma cells (28). These facts further complicate the issue of whether PNPase acts as a 3′–5′ exonuclease of mRNAs in mitochondria.

The mitochondrial RNA degradosome (mtEXO) in *Saccharomyces cerevisiae* consists of Dss1p, which functions as a 3′–5′ exonuclease (RNase II-like), and Suv3p, which acts as a DExH/D RNA helicase (29). Recombinant protein of the human homolog of SUV3 forms a stable complex with PNPase, which degrades RNA in the 3′–5′ direction *in vitro* (30). Overexpression of the dominant negative mutant of *SUV3* (or *SUPV3L1*) results in the elongation of the poly(A) tail of mRNAs and the accumulation of aberrant transcripts from the antisense strand,

indicating the involvement of SUV3 in mitochondrial mRNA degradation (31).

In this article, we provide evidence that the LRPPRC/SLIRP complex suppresses mRNA degradation mediated by PNPase and SUV3 and promotes polyadenylation of mRNA mediated by mitochondrial poly(A) polymerase MTPAP *in vitro*.

MATERIALS AND METHODS

Cell culture

HeLa cells were grown in Dulbecco's modified Eagle medium (DMEM) supplemented with 10% fetal bovine serum at 37°C under a humidified atmosphere with 5% CO_2.

Quantitative reverse-transcription real-time polymerase chain reaction

Total RNA was isolated from cells using TRI Pure (Roche), according to the manufacturer's instructions. RNA was treated with DNase I (Promega) for 30 min at 37°C. cDNA was synthesized using the Transcriptor First Strand cDNA Synthesis Kit (Roche). Random N6 primers or gene-specific reverse primers [quantitative polymerase chain reaction (qPCR) reverse primers] were used for cDNA synthesis. For mitochondrial tRNAs, qPCR reverse primers were used for the first strand cDNA synthesis. Amplification of cDNA was monitored with the LightCycler 480 SYBR Green I Master (Roche) on a LightCycler 480 (Roche), according to the manufacturer's instructions. The sequences of the qPCR primers are listed in Supplementary Table S1.

Absolute quantification of human mitochondrial mRNAs in HeLa cells

For absolute quantification of mRNAs, *in vitro* transcribed mRNAs were prepared as external standards for qRT-PCR. The cDNAs for all mitochondrial mRNAs were amplified by RT-PCR from the total RNA of HeLa cells using the primers listed in Supplementary Table S1, preceded by a T7 class III promoter sequence (32). All 11 mitochondrial mRNAs were transcribed by T7 RNA polymerase *in vitro* (32) and purified by denaturing polyacrylamide gel electrophoresis. The isolated mitochondrial mRNAs were quantified by measuring the optical density at 260 nm. HeLa cells grown in five dishes ($4.86 \pm 0.26 \times 10^6$ cells/dish) were washed with phosphate-buffered saline (PBS) and lysed by adding TRI Pure (Roche) directly to the dishes. Twenty micrograms of total RNA from *Echerichia coli* was added to this mixture as a doped marker to estimate the recovery rate of total RNA. Total RNA was isolated from the cells according to the manufacturer's instructions and dissolved in 100 µl of water. The recovery rate of total RNA from HeLa cells was calculated by analyzing the loss of *E. coli gapA* mRNA in the doped marker by qRT-PCR. The total RNA (5 µg) from each of the five dishes was treated with DNase I (Promega), and a portion of the total RNA was subjected to cDNA synthesis using gene-specific reverse primers for all mitochondrial mRNAs (qPCR reverse primers listed in Supplementary Table S1). qRT-PCR was conducted as described above. The copy number of each mitochondrial mRNA in the total RNA from one HeLa cell was determined using the calibration line of each mRNA, which was generated by quantifying the amount of *in vitro* transcribed mRNAs by qRT-PCR. The recovery rate of RNA extraction was also taken into account to determine the copy numbers.

RNAi

siRNAs targeted to *LRPPRC*, *SLIRP*, *PNPase*, *PDE12*, *SUV3* and *luciferase* were designed using the siRNA design algorithm 'siExplorer' (33). The siRNAs used here are listed in Supplementary Table S1. HeLa cells (2.5×10^5) were transfected with 60 pmol of siRNA (5 nM, final concentration) using Lipofectamine RNAi Max (Invitrogen).

Inhibition of mitochondrial transcription

Mitochondrial transcription was inhibited, as previously described (5). Cell culture medium was replaced with DMEM supplemented with 10% fetal bovine serum and 500 $ng \cdot ml^{-1}$ of ethidium bromide, and total RNA was collected at 0, 1, 2, 4 or 6 h after the initiation of mitochondrial transcription inhibition.

Western blotting

Cells were washed with PBS and collected with a rubber scraper. After centrifugation at 1000*g* for 2 min, cell pellets were resuspended in 100 µl of lysis buffer [100 mM NaCl, 10 mM Tris–HCl (pH 7.4), 2.5 mM $MgCl_2$, 0.2% sodium dodecyl sulfate (SDS) and protease inhibitor cocktail (Roche)] and sonicated with a Sonifier 450D (Branson) for 5 s at power 3. Lysates were clarified at 20 000*g* for 10 min, and the samples were then resolved by SDS polyacrylamide gel electrophoresis (SDS–PAGE) and transferred to a nitrocellulose membrane using an iBlot transfer apparatus (Invitrogen). Membranes were blocked with 10% Sea Block blocking buffer (Pierce) in Tris-buffered saline and probed with primary antibodies. Primary antibodies for LRPPRC (Santa Cruz), SLIRP (Santa Cruz) and β-actin (Sigma) were used at a dilution factor of 1:200, 1:100 and 1:5000, respectively. Horseradish peroxidase-conjugated anti-mouse (Dako) and anti-rabbit (Jackson ImmunoResearch Laboratories) secondary antibodies were used at 1:2000 and 1:15 000, respectively. Proteins were illuminated using ECL Plus (GE Healthcare) and visualized with an ImageQuant LAS4000 mini (GE Healthcare).

Immunoprecipitation

Approximately 5×10^6 HeLa cells were washed by PBS and crosslinked by incubation in PBS containing 0.15% formaldehyde for 10 min at room temperature (34). The crosslinking reaction was quenched with 0.25 M glycine (final concentration). Cells were washed with PBS and collected by a rubber scraper, followed by centrifugation at 1000*g* for 2 min. The cell pellet was resuspended in

1 ml of buffer A [100 mM NaCl, 10 mM Tris–HCl (pH 7.4), 2.5 mM $MgCl_2$, 0.1% SDS, 0.5% sodium deoxycholate, 1% Triton X-100 and 1 mM dithiothreitol (DTT)] containing Complete protease inhibitor cocktail (Roche) and SUPERaseIN (Ambion) and passed through a 25-gauge needle 10 times. Lysates were centrifuged at 20 000 *g* for 25 min and the supernatant was incubated with Protein G agarose for 1 h. The samples were then centrifuged and the supernatant was incubated with LRPPRC antibody (Santa Cruz)-bound Protein G beads for 2 h. The antibody beads were washed five times with buffer A. After immunoprecipitation, the cell lysate and precipitants were decrosslinked by incubating the precipitants in 100 µl of crosslink reversal buffer [50 mM Tris–HCl (pH 7.4), 5 mM ethylenediaminetetraacetic acid (EDTA) (pH 8.0), 1% SDS and 10 mM DTT] at 70°C for 30 min. For the experiment in Figure 3B, immunoprecipitation was conducted in the same way as described above, except that cells were transfected with the LRPPRC-Flag vector (as described below) and anti-Flag M2 agarose (Sigma) was used instead of LRPPRC antibody-bound beads.

Analysis of RNA fragments bound to the LRPPRC/SLIRP complex

The Human Gateway entry clone (35) and DEST12.2 Flag plasmid were used in this study. The LRPPRC expression vector was generated by LR reaction of pDEST12.2 Flag and Entry clone FLJ43793AAAN using LR Clonase (Invitrogen). The C-terminally Flag-tagged LRPPRC vector was generated by changing the stop codon of the LRPPRC expression vector to Tyr, using the primers 5′-actcttcttatgacccagctttcttg-3′ and 5′-caagaaagctgggtcataagaagagt-3′. Approximately, 2×10^7 HeLa cells were transfected with the LRPPRC-Flag expression vector using FuGENE HD (Roche). At 40 h post-transfection, the cells were crosslinked, collected, lysed and precleared and immunoprecipitated (as described above) using anti-Flag M2 affinity beads. Subsequently, the antibody beads were washed twice with buffer B [100 mM NaCl, 10 mM Tris–HCl (pH 7.4), 0.1 mM EDTA, 1 mM DTT], followed by fragmentation of RNAs by incubation in 100 µl of buffer B containing 5 units/µl RNase T1 (Epicentre) and 10 µg/ml RNase A (Ambion) for 1 h at 37°C. The antibody beads were then washed four times with buffer A. 100 µl of crosslink reversal buffer and 10 µl of Proteinase K (Roche) were added, and the beads were incubated at 55°C for 30 min and then at 70°C for 20 min. One milliliter of TRI Pure (Roche) was added, and the RNA fragments were extracted according to the manufacturer's instructions, except that ethanol precipitation was performed overnight at −80°C. The RNA precipitate was dephosphorylated by bacterial alkaline phosphatase A19 (Takara) and then extracted by phenol–chloroform–isoamyl alcohol (PCI) (Nacalai) and precipitated with ethanol. The adaptor DNA (5′-p-atgtgagatcatgcacagtcata-NH_2-3′) was ligated at the 3′ ends of isolated RNA fragments, as described in the poly(A) tail length assay. Next, 3′ adaptor-ligated RNA fragments were extracted by PCI and precipitated with ethanol. The fragments were resolved by denaturing PAGE and stained with SYBR Gold (Invitrogen). Fragments larger than 20 nt were excised, and the RNA fragments were eluted from the gel and ethanol precipitated. The 5′ ends of 3′ adaptor-ligated RNA fragments were phosphorylated by T4 polynucleotide kinase (Toyobo), and the RNA solution was put through a NAP5 column (GE Healthcare) to remove excess ATP and then precipitated with ethanol. The 5′ ends of the RNA fragments were ligated to 5′ adaptor DNA (5′-ctcctggcaaaaggtcagag-3′) using T4 RNA ligase, as described in the mt poly(A) length assay, and were then extracted by PCI and ethanol precipitated. The 5′ and 3′ adaptor-ligated RNAs were resolved by denaturing PAGE and stained with SYBR Gold. Fragments larger than 50 nt were excised from the gel, eluted and recovered by ethanol precipitation. Adaptor-ligated RNA fragments were reverse-transcribed by Transcriptor reverse transcriptase (Roche). cDNAs were amplified by Taq polymerase (Toyobo) with the primers 5′-ctcctggcaaaaggtcagag-3′ and 5′-gactgtgcatgatctcacat-3′. The PCR product was resolved by native PAGE and stained with Mupid Blue (Takara). PCR products larger than 50 bp were excised from the gel, eluted, collected by isopropanol precipitation and cloned into plasmids using the TA cloning kit (Invitrogen) for DNA sequencing.

Poly(A) tail length assay

The assay is based on and altered from the method described by Temperley *et al.* (36). An adaptor DNA oligonucleotide was ligated to the 3′ termini of total RNA (5 µg) by T4 RNA ligase (New England Biolabs) at 37°C for 3 h, according to the manufacturer's instructions. The ligated RNA was isolated by TRI Pure (Roche) and isopropanol precipitation and then reverse-transcribed using the First Strand cDNA Synthesis Kit (Roche) with the anti-adaptor primer. A first round of PCR (27 cycles) was carried out using a gene-specific upper primer and the anti-adaptor primer, followed by a second round of 10-cycle PCR using an inner anti-adaptor primer and a gene-specific lower primer. Finally, the PCR product was resolved by 10% polyacrylamide gel electrophoresis in TBE buffer, dyed with SYBR Gold (Invitrogen) and visualized with an FLA-7000 (Fujifilm). All oligo-DNAs are listed in Supplementary Table S1.

Quantification of human LRPPRC protein in HeLa cells

HeLa cells grown in three dishes ($2.76 \pm 0.20 \times 10^6$ cells/dish) were washed with PBS and lysed by direct addition of lysis buffer [100 mM NaCl, 10 mM Tris–HCl (pH 7.4), 2.5 mM $MgCl_2$, 0.2 % SDS and protease inhibitor cocktail (Roche)] to the dishes. Cell lysates were collected from dishes with a rubber scraper and sonicated with a Sonifier 450D (Branson) for 24 s.

For LRPPRC protein quantification, recombinant His-LRPPRC was prepared as an external standard for western blotting. The cDNA for *LRPPRC* without the mitochondria-targeting signal (amino acid residues 60-1394) was amplified by RT-PCR of the total RNA from HeLa cells using the primers 5′-caacgtgctagcgccattgctgccaaagaaa-3′